ENGINEERING RESEARCH INSTITUTE
THE UNIVERSITY OF MICHIGAN
ANN ARBOR

Technical Report

CAMERA CALIBRATION AND ABSOLUTE CHECK ON PHOTOGRAMMETRIC TILT DETERMINATION USING STAR TRAILS

Eldon Schmidt

Edward Young

Project 1699-1

DEPARTMENT OF THE AIR FORCE
WRIGHT AIR DEVELOPMENT CENTER
WRIGHT-PATTERSON AIR FORCE BASE, OHIO
CONTRACT NO. W33(038)ac-15318
PROJECT NO. 54-650A-460

July 1955

TABLE OF CONTENTS

ABSTRACT

Technically, this investigation is aimed at finding the accuracy of the photogrammetric method as used by this project in evaluating the performance of airborne instruments in flight. The extreme accuracies of stellar positions are utilized in photogrammetric applications. This involves methods of reproducing star images in an advantageous manner and reducing the stellar positions to corresponding planar positions. There are given, in addition to the general procedure and instrumentation, two specific photogrammetric applications using these star images. One is a method of checking the accuracy of tilt values in a physical sense and the other a method of camera calibration.

OBJECT

The object of this project is to determine methods of photogrammetric reductions for aerial defense purposes.

GENERAL INFORMATION

Star photography offers an excellent opportunity for studies in photogrammetry. Among the many reasons for this are:

1. The angular positions of the stars are known to an accuracy of at least 0.1 second of arc. This accuracy results from many years of observation by the observatories of the world. Thus, photogrammetrically the stars can be considered an almost perfect control system with respect to accuracy.

2. The star images on a photograph are ideal from the point of view of photogrammetry as they represent point sources of light. Such images can be measured with very high accuracy on a film or plate.

3. Such a control system is universal as it can be used from any point on the surface of the earth. Among the disadvantages can be numbered:

(1) Due to the diurnal motion, the control system is not stationary.
(2) Because of large differences in brightness or magnitude all images are not reproduced equally.
(3) The stars are effectively positioned at random and hence exhibit no symmetries.
(4) The stars are displaced from their given positions by refraction in the atmosphere.

Star-trail photography takes advantage of all the favorable conditions while at the same time eliminating to a large degree disadvantages (1) and (3). Star trails are produced by leaving the camera shutter open for long periods of time causing the star images to traverse the photographic plane due to their diurnal motions. The exact angular position of any given star with respect to the camera's position can be found for any given instant of time if the astronomical position of the camera is known. Thus, disadvantage (1) is overcome if an exact time correlation is established along with the camera's position. It should be mentioned here that the camera's position refers to the astronomical latitude and longitude of the camera. Also along each trail there are now an infinite number of control points increasing greatly the control density. For an exposure of several hours all areas of the photographic plane are covered. This permits selection of almost any symmetry desired, overcoming

disadvantage (3). Disadvantage (2) is caused principally by halation effects in the images of the brighter stars. However, these images are still superior to those of finite targets as used in conventional photogrammetry. Disadvantage (4) presents no serious difficulties as the effects of atmospheric refraction on star positions have been determined by astronomers to almost any degree of accuracy desired. Thus, this source of error can be removed.

From a practical point of view it is necessary to cause identifying marks to appear along the trails for the purpose of time correlation. This is most easily accomplished by closing the shutter for a few seconds at some specified time causing a break to appear in the trail. The shutter must be open long enough so that halation effects will not close up the gap in the trail. For the work done at this project a 5- to 7-second interval was found to produce satisfactory breaks even in the stars near the pole where diurnal motion is the least.

These breaks then constitute the control points for reduction. An example of such a system of star trails appears in Photograph I.

LATITUDE AND LONGITUDE POSITION OF THE CAMERA STATION

The geodetic position of the camera station was determined by triangulation. The astronomical position was determined by stellar observations. The difference between the two is the deflection of the vertical at the station. In the section "Absolute Check on Tilt Determination" described later, the astronomical position was used in the final computations: When the geodetic position is used in the photogrammetric tilt computations a correction for the deflection of the plumb line must be applied to the photogrammetric tilt since these measurements are referred to the normal of the spheroid, while the theodolite measurements of the tilt described later are referred to a surface perpendicular to the plumb line. It is simpler to use the astronomical position in the photogrammetric tilt computations than to apply the correction.

The camera station, located in building 360 on the east side of Willow Run Airport, was chosen after the ground stability was checked with respect to possible shock from aircraft landing on the airfield. Intervisibility with three U.S. Coast and Geodetic Survey stations was another factor in the selection. A welded steel tower set on a reinforced concrete slab in a pit with mastic between the slab base and pit walls was used for the camera mount. The following U.S. Coast and Geodetic Survey stations were visible from the camera station: Airport Beacon, Ford Bomber Plant (now GM) Tank, and Leland Water Tank. The latitude and longitude as well as the plane coordinates on the Michigan State grid of these stations were obtained from the USC and GS, their positions having been determined by intersections from first-order triangulation stations.

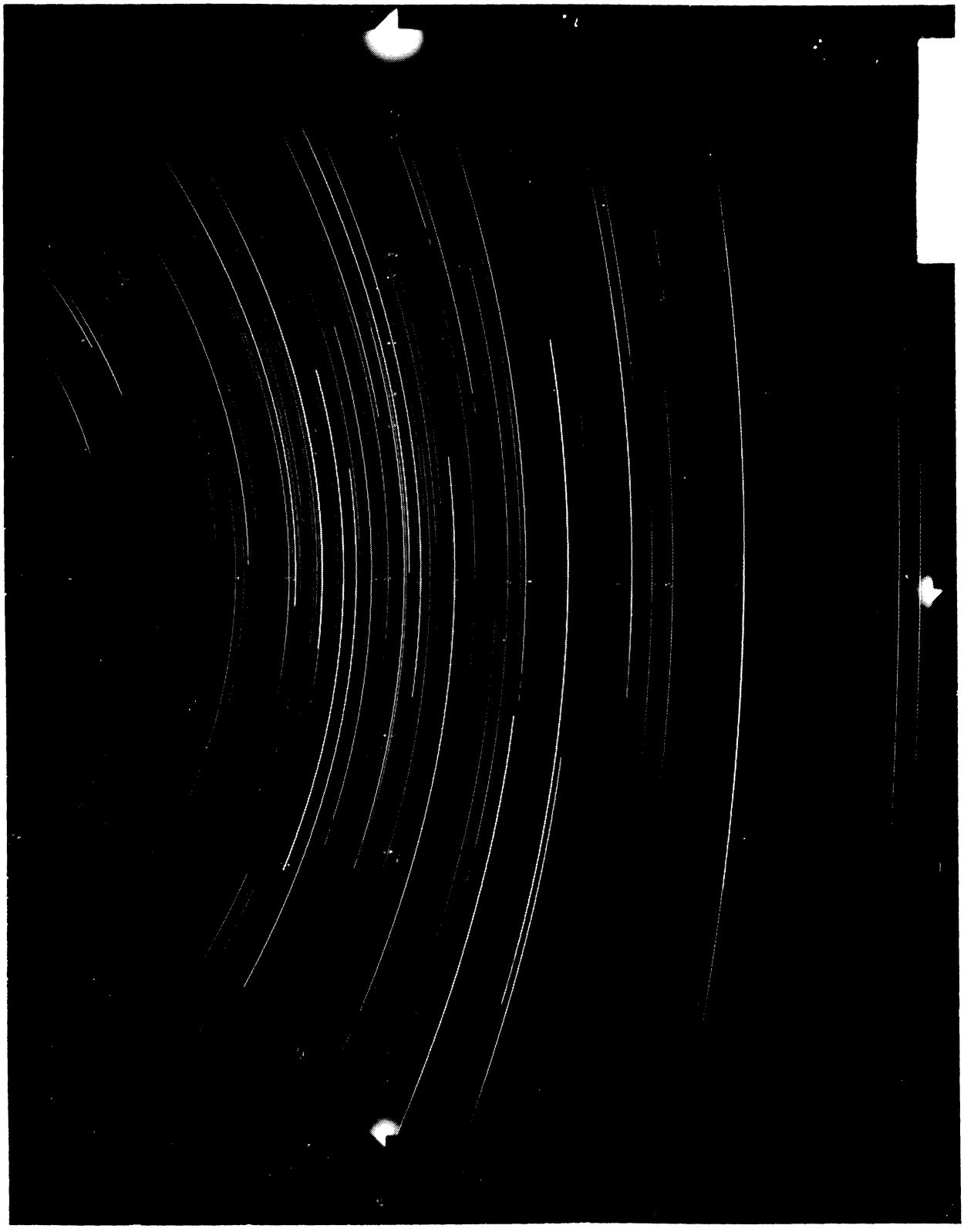

Photograph I (One fiducial mark was cut off in reproduction.)

GEODETIC POSITION

To obtain the geodetic position of the camera station, a three-point method was used (Fig. 1). The angles P' and P" were measured. Although the average probable error in the measured angles was ± 1.29 seconds of arc, the figure when tested was weak and extremely sensitive to slight changes in the measured angles. Since it was possible to occupy station Airport Beacon as an eccentric station it was decided to do so, using the distance from Airport Beacon to the camera station, obtained from the three-point solution, to reduce the angle to center and solve the problem as a traverse. The grid azimuths obtained were reduced to geodetic azimuths and the latitude and longitude at the camera station and the back azimuth of the lines were computed. The computations for geodetic position will be omitted since it is a standard method and can be found in any geodesy textbook and in USC and GS special publications. The geodetic position of the camera station was computed from two stations giving the following values:

Computed from Airport Beacon
latitude (ϕ) = 42°-14'-17".053
longitude (λ) = 83°-30'-49".186
Computed from Ford Bomber Plant (now GM) Tank
ϕ = 42°-14'-17".060
λ = 83°-30'-49".190

The difference in the latitude values of 0.007 second of arc is equivalent to 0.71 foot in ground position. The difference in the longitude values of 0.004 second of arc is equivalent to 0.29 foot on the ground in this latitude. The value obtained over the shorter line from Airport Beacon was taken as the best value.

ESTABLISHING MERIDIAN AT THE CAMERA STATION

From the back azimuth obtained in the computations between Ford Bomber Plant Tank and the camera station, angles were turned to establish true north. The established line was then checked by observations on Polaris at elongation. A very close agreement was found between the two azimuths. This indicates a Laplace point in the area.

ASTRONOMICAL POSITION OF THE CAMERA STATION

As already stated, the difference between geodetic position and astronomical position is the deflection of the plumb line at the station. In

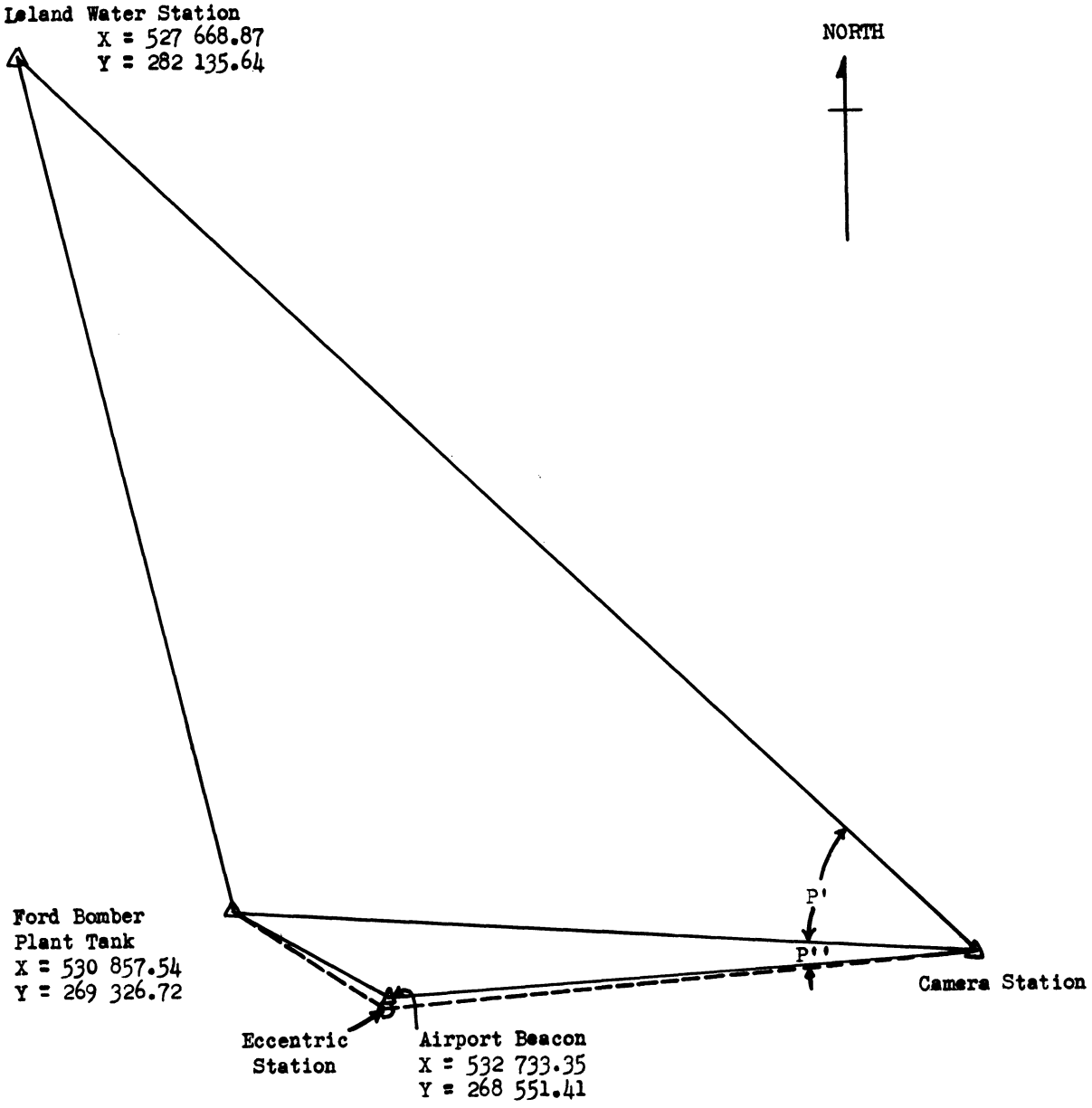
Leland Water Station
X = 527 668.87
Y = 282 135.64
NORTH
Ford Bomber
Plant Tank
X = 530 857.54
Y = 269 326.72
P'
P''
Camera Station
Eccentric
Station
Airport Beacon
X = 532 733.35
Y = 268 551.41

Fig. 1

the absolute check on photogrammetric tilt accuracy discussed later, a correction for this deflection must be applied if the computations are based on geodetic position. Therefore, the astronomical position of the camera station was determined by the following described methods.

LONGITUDE BY MERIDIAN PASSAGE OF STARS

A theodolite having a least reading of 1 second of arc and equipped with a 5-second-per-2-mm striding level and a Horrebow level (horizon level) having the same sensitivity was used in the stellar observations. A typical star list for one night's observing is shown in Table 1. The approximate time of meridian passage was computed for each star as well as the approximate zenith distance. All observed stars were later computed for their exact time of passage for the geodetic longitude of the meridian and compared with the recorded time of passage to obtain the deflection of the vertical in this direction. Three individual timed sights were taken to each star (three vertical cross-hairs) and the mean value used. The theodolite was used equally in the direct and inverted position to eliminate instrumental errors. In all star observations the time of passage was recorded on a brush oscillograph tape superimposed on the time signals from radio station WWV of the Bureau of Standards. The instrumentation used was the same as that used in the calibration work of Fig. 2 except the cams were not used. Instead, a microswitch at the theodolite was used to send a pulse through a 6-volt battery circuit to the brush recorder. The brush was run at a speed of 25 mm per second. This permitted scaling the time of each pulse to the nearest 0.01 second. In addition to recording the time of meridian passage, the zenith distance was measured to obtain latitude. This is not an approved method for determining latitude due to the larger correction for atmospheric refraction at greater zenith distances. In our case, however, because of the large number of observations the mean value proved to be a good check on the "equal zenith distance" method used.

Error Consideration in the Longitude Determination.—It is possible to investigate the error of each longitude determination. It will be composed of the following:

Constant errors

1. Error in time signals; negligible
2. Error in meridian; ± 1.5 seconds of arc, 0.10 second of time
3. Error in collimation; balanced out

Random errors

4. Error in meridian setting; ± 1.0 second of arc, 0.07 second of time
5. Error in determining the exact instant of passage; ± 0.14 second of time
6. Error in reading the oscillograph tape; ± 0.01 second of time
7. Error in horizontal axis; correction applied
8. Refraction; ± 1.0 second of arc

TABLE 1. TYPICAL STAR LIST

Meridian Passage, 26 August 1954

Longitude of theodolite station (49.47 ft west of camera station) = $5^h34^m03^s.324$

Name of Star	Approximate Time of Passage (EST)	Approximate Zenith Distance
ξ Serpentis	$19^h50^m09^s$	57°34'
58 Ophiuchi	19-55-51	63-21
χ Sagittarii	19-59-50	70-00
ν Ophiuchi	20-11-38	51-59
γ Sagittarii	20-17-59	72-39
μ Sagittarii	20-27-57	63-17
δ Sagittarii	20-33-09	72-02
λ Sagittarii	20-40-11	67-39
α Scuti	20-47-45	50-30
δ Scuti	20-54-46	51-19
ϕ Sagittarii	20-57-28	69-14
β Scuti	21-00-44	47-01
σ Sagittarii	21-07-25	68-33
ξ Sagittarii	21-09-58	63-22
λ Aquilae	21-18-46	47-10
π Sagittarii	21-21-59	63-18
20 Aquilae	21-26-07	50-15
ν Sagittarii	21-34-01	58-15
186 Sagittarii	21-39-27	72-04
52 Sagittarii	21-49-20	67-13
58 Sagittarii	21-54-45	58-26
56 Sagittarii	21-58-31	62-06
51 Aquilae	22-03-05	53-07
61 Sagittarii	22-10-10	57-49
62 Sagittarii	22-14-39	70-02
θ Aquilae	22-23-42	43-12
α^1 Capricorni	22-29-52	54-55
α^2 Capricorni	22-30-16	54-52
β Capricorni	22-33-11	57-09
69 Aquilae	22-41-59	45-15
29G Capricorni	22-44-36	52-13
ν Capricorni	22-53-03	60-30
ϵ Aquilae	22-59-53	51-54
μ Aquarii	23-04-51	51-24
64G Capricorni	23-09-46	58-26
11 Aquarii	23-12-47	47-08
θ Capricorni	23-17-30	59-39
ν Aquarii	23-20-57	53-47
58G Microscopii	23-25-12	70-03
ι Capricorni	23-34-17	59-16
ξ Capricorni	23-38-37	64-51
β Aquarii	23-43-42	48-00
ξ Aquarii	23-49-51	50-18
γ Capricorni	23-52-05	59-06
δ Capricorni	23-59-01	58-34

Discussion of Errors in Longitude Determination.—

1. Examination of the reports "Deviations and Adjustments of Standard Frequencies and Time Signals as Broadcast by the National Bureau of Standards," Station WWV, for the specific dates shows that the small error of a few milliseconds is negligible when compared with errors from other sources.
2. The probable error of two nights' observations on Polaris at elongation was ± 1.5 seconds of arc = 0.1 second of time.
3. The error in collimation was largely elimated by using an equal number of direct and indirect pointings with the theodolite.
4. Meridian setting ± 1 second of arc - 0.07 second of time.
5. The error in determining the exact instant of star passage, that is, when the star is exactly bisected by a vertical cross-hair, is more difficult to obtain. Examination of the passage of 25 consecutive stars across the three vertical cross-hairs gave the following: The mean time was computed and compared with the value obtained from the middle cross-hair. For the 25 stars the mean difference between the value for the middle hair and that obtained from the mean of three cross-hairs was 0.14 second of time. The time recorded on the middle hair showed 10 stars to be 0.133 second early and 15 stars 0.147 seconds of time late when compared with the mean.
6. The oscillograph tape was run at a speed of 25 mm per second permitting reading to ± 0.01 second of time.
7. Error in horizontal axis: A 5-second-per-2-mm striding level was read during each observation and a correction applied when required. By the law of error propagation the probable error of a single observation is found to be 0.16 second of time = 2.4 seconds of arc. The probable error 1/n th of this sum equals 0.16 second/$\sqrt{n}$ time or 2.4/$\sqrt{n}$ seconds of arc which is the probable error of the arithmetical mean of n observations. For n = 25 the probable error of the mean equals 0.16 seconds/$\sqrt{25}$ equals ± 0.032 second of time equals 0.480 second of arc or the equivalent to 36.10 feet on the ground. As already stated, the probable error of the mean in longitude determination was 23.5 feet.

LATITUDE BY EQUAL ZENITH DISTANCES

A more precise way to obtain latitude is by observing pairs of stars having nearly equal zenith distances with one star north and one star south of the zenith (Table 2). When the zenith distances are 15 to 20 degrees the refraction correction is not only small but varies only about 1 second per degree. The latitude (ϕ) is computed from

$$\phi = 1/2(\delta_1 + \delta_2) + 1/2(Z_1 + Z_2)$$

where δ_1 and δ_2 are the declination of the stars and Z_1 and Z_2 the zenith distances corrected for refraction.

TABLE 2. TYPICAL STAR LIST

Latitude by Equal Zenith Distance Stars, 16 November 1954

Name of Star	Magnitude	Approximate Time of Passage (EST)	Approximate Zenith Distance
α Cephi	2.6	$18^h09^m30^s$	20°09'N
2 Pegasi	4.76	18-20-12	18-47 S
13H Cephi	5.97	18-38-40	15-03 N
16 Pegasi	5.05	18-43-05	16-31 S
π Pegasi	4.38	19-00-00	9-16 S
β Lacertae	4.58	19-13-56	9-46 N
38 Pegasi	5.51	19-19-56	9-56 S
α Lacertae	3.85	19-21-21	9-48 N
η Pegasi	3.10	19-32-47	12-15 S
μ Pegasi	3.67	19-39-57	17-53 S
β Pegasi	2.61	19-53-41	14-23 S
Bradly 3077 Cassiopeiae	5.65	20-03-10	14-41 N
τ Pegasi	4.55	20-10-28	18-47 S
4 Cassiopeiae	5.20	20-14-37	19-48 N
θ Piscium	4.45	20-17-41	36-06 S
γ Cephei	3.42	20-29-30	35-09 N
41 Cephei	5.02	20-37-30	25-20 N
∅ Pegasi	5.23	20-41-55	23-25 S

The values obtained for the astronomical position of the camera station are given below along with the geodetic position to show the value obtained for the deflection of the vertical.

Geodetic latitude 42°14'17".053
Astronomical latitude 42°14'11".411

The difference of 5.642 seconds of arc is equivalent to 572 feet on the ground.

Geodetic longitude $5^h34^m03^s.280$
Astronomical longitude $5^h34^m03^s.091$

The difference of 0.189 second of time is equal to 2.835 seconds of arc and corresponds to 213 feet on the ground in this latitude.

In order to get a further check on the deflection in this area the geodetic position of the meridian circle 10 miles away at the University of Michigan observatory was determined from a nearby geodetic station. When compared with the astronomical position the difference was found to be 6.3 seconds of arc (637 feet) in latitude and 4.9 seconds of arc (367 feet) in longitude. The differences obtained are in the same direction as those found at the camera station but differ by 65 feet in latitude and 154 feet in longitude. If one can assume that no appreciable change takes place in 10 miles, the difference of 65 feet is reasonable since our average probable error in latitude was ± 75 feet. On the same assumption the difference of 154 feet is large since our average probable error in longitude was ± 23.5 feet. On the above assumption this would indicate a constant error of about 2 seconds of arc in the meridian which of course would not show in the residuals.

The latitude and longitude were determined by solving each night's work separately and determining the probable error. A star having a large residual was discarded. This was usually a case of misidentification giving discordant values for both latitude and longitude.

Error Consideration in Latitude Determination.—With the exception of refraction, the errors discussed in the longitude determination have little effect on the latitude determination which involves a measurement of the zenith distance. The more important errors are listed below.

1. Errors in leveling the bubble and reading the vertical circle; ± 1.0 second
2. Refraction; ± 1.0 second
3. Errors in graduated circle assumed 0
4. Bisection of the star with horizontal cross-hair assumed ± 1.0 second

Again by the law of error propagation the probable error of a single observation is 1.73 seconds of arc and the probable error of the arithmetic mean of n observations is $1.73/\sqrt{n}$.

Discussion of Errors in Latitude Determination.—

1. The combined probable error of releveling the bubble and reading the vertical circle was found by a series of readings with the telescope in the same position and the bubble releveled before each reading. The probable error of the mean of the series was 0.15 second of arc and the probable error of a single observation was 0.47 second of arc. These readings were made with the advantage of daylight, the instrument shaded from the direct rays of the sun, and with ample time to observe the bubble. Under actual observation conditions, the error in

a single observation will be greater than 0.47 second; therefore, a value 1.0 second has been assumed.

2. When the zenith distance of a star is 15 to 20 degrees, the refraction correction is small and varies about 1 second per degree. For 65 degrees the variation is about 5-1/2 seconds per degree. Even for the latter case there should be no difficulty in obtaining refraction to ± 1.0 second.
3. The errors in the graduated circle of the theodolite are not known but they can be assumed to be small as compared to other errors.
4. Since the star is a point source of light, at infinity, bisection with the horizontal cross-hair should not exceed ± 1.0 second of arc. As already stated the probable error of the mean of all latitude observations was 0.75 second of arc or the equivalent of 75 feet on the ground. Since the mean value of the latitude varied different nights there is little doubt that there are errors in the determination that are not revealed in the residuals. However, it is unlikely that the mean of all observations will be in error by more than ± 75 feet.

INSTRUMENTATION

THE CAMERA

The camera should be clamped in a rigid structure where it is protected from shock and accidental motion. Space should be provided for loading and any equipment desired for experimentation. At this project a T-11 camera was used and mounted on a steel tower. This tower is set on a concrete base in a building to protect it from the weather. The camera installation is in an unheated part of the building which is open enough to assure the same temperature inside as outside; this holds the temperature gradients as uniform as possible. Access to the sky is provided by an opening in the roof. The mount and camera are illustrated in Photographs II and III. The camera is equipped with a plate holder since glass plates are generally preferable to film in this type of work. The camera shutter is left open and takes no part in the experiment. This is a further protection against shock to the camera during exposure.

As in all photogrammetric work the fiducials are vital as reference axes fixed in the camera. These must also be reproduced on the plate during exposure. Since the T-11 is equipped with artificial illumination for the fiducials, this was no problem for our work. However, many cameras depend on natural illumination through the lens. In this case it is necessary to provide some system of illumination. Since this is discussed thoroughly in reference 3, it will not be discussed further here.

The camera is equipped with an external shutter to replace the unused internal shutter. The shutter mechanism must not touch the camera installation

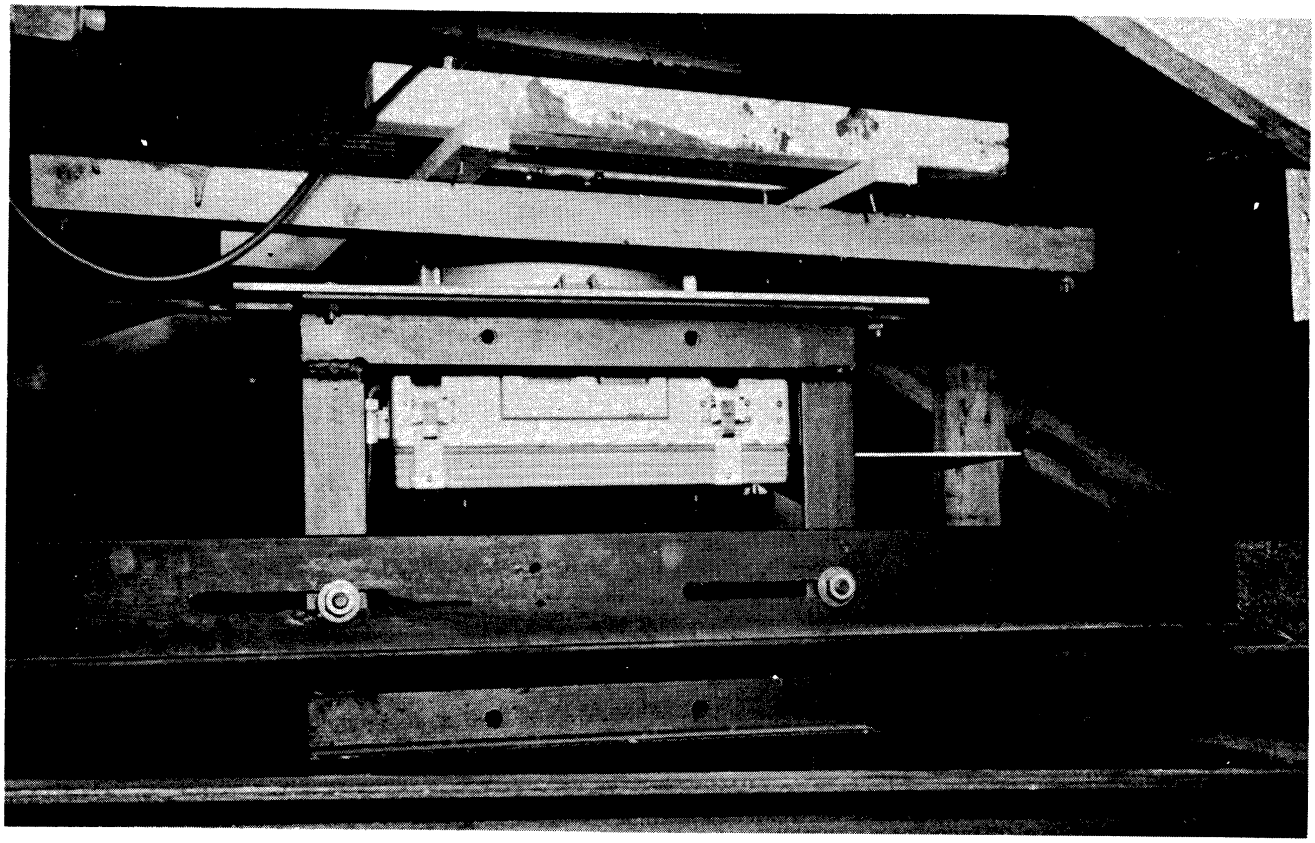

Photograph II. This shows the camera in place with the shutter also in position. Note that the shutter is suspended from the building and does not touch the camera. The top of the tower of Photograph III appears at the bottom. The T-5 camera is clamped rigidly in an angle-iron mount.

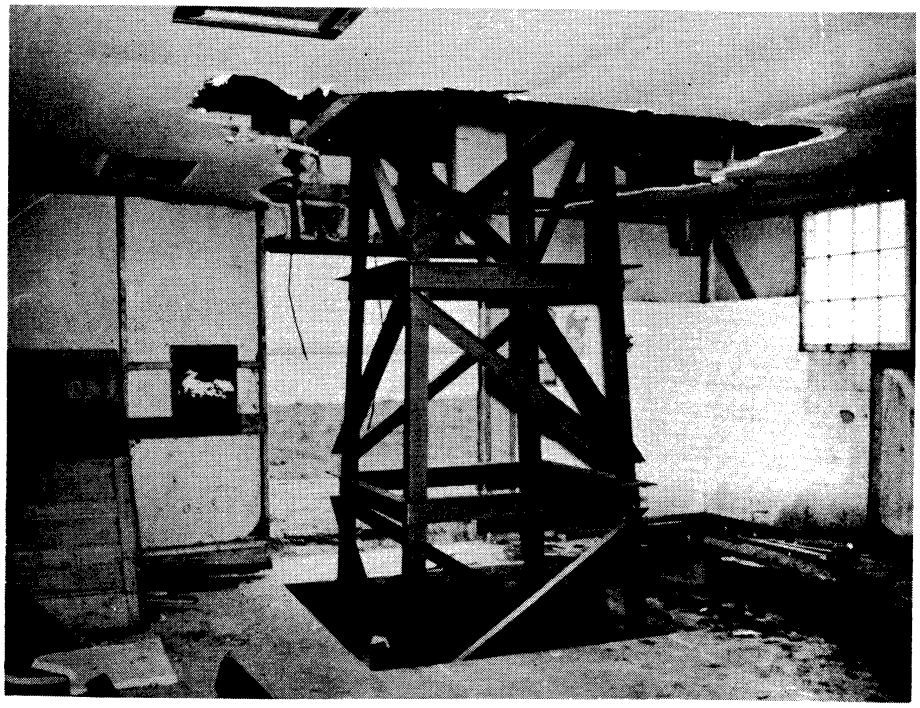

Photograph III. This is a view of the tower showing its construction.

as its shock would then defeat its purpose. It is vital that the camera not be disturbed during exposure. In our case the solenoid-driven shutter illustrated in Photograph IV is mounted on the building independent of the camera installation. There is no light leak problem with such a shutter as exposure is made at night. It is necessary that no artificial lights shine directly on the camera from the side or from above.

TIME CORRELATION

It is necessary to establish an exact time correlation with each break on the photograph. This is done as follows: The source of exact time is the time signal broadcast by station WWV. These signals are amplified and reproduced on a brush oscillograph where they appear as sharp pips. The pulses that activate the shutter solenoids are superimposed on the same trace. Thus, the desired time correlation appears on the tape of the oscillograph.

A block diagram of the wiring of the equipment as used on this project is shown in Fig. 2. The filter amplifier circuit is shown in Fig. 3. The time sequence of events is illustrated on the sample tape of Photograph V. By this method the time can be found to about 0.1 second. The three cams, mounted on one shaft, are driven by a 1-rpm motor producing one break per minute along each trail. Cam 1 activates the brush oscillograph motor. This is to conserve tape by operating the oscillograph only during the period covering the break; cam 2 activates the relay system closing the shutter; and cam 3 activates the system opening the shutter. The time delays in the system are short enough to be imperceptible on the time scale provided by the tape and may be ignored. In Photograph V the method of finding the exact time that the star in question was at the center of the break is illustrated. The center of the break is used for reasons of symmetry in measuring. In the photograph the appearance of a typical break is shown with the time correlation.

This equipment with the exception of the shutter is in a separate part of the building. This is to provide heated quarters for the operators who must sometimes spend an entire evening getting one good exposure.

PLATES AND DEVELOPMENT

The plates used by this project were Kodak Tri-X, Panchromatic Type B. Plate dimensions are 9-1/2 x 9-1/2 x 1/4 inches. These thick plates were used to hold the plane of the emulsion as flat as possible. Thin plates might bow depending on the type of support in the plate holder. Panchromatic plates are preferable as they take fullest advantage of the available stellar spectrum.

Development was made in D-11 for 5 minutes at 68°F. After fixing and washing, the plates were dried in a horizontal position to hold emulsion shifts to a minimum.

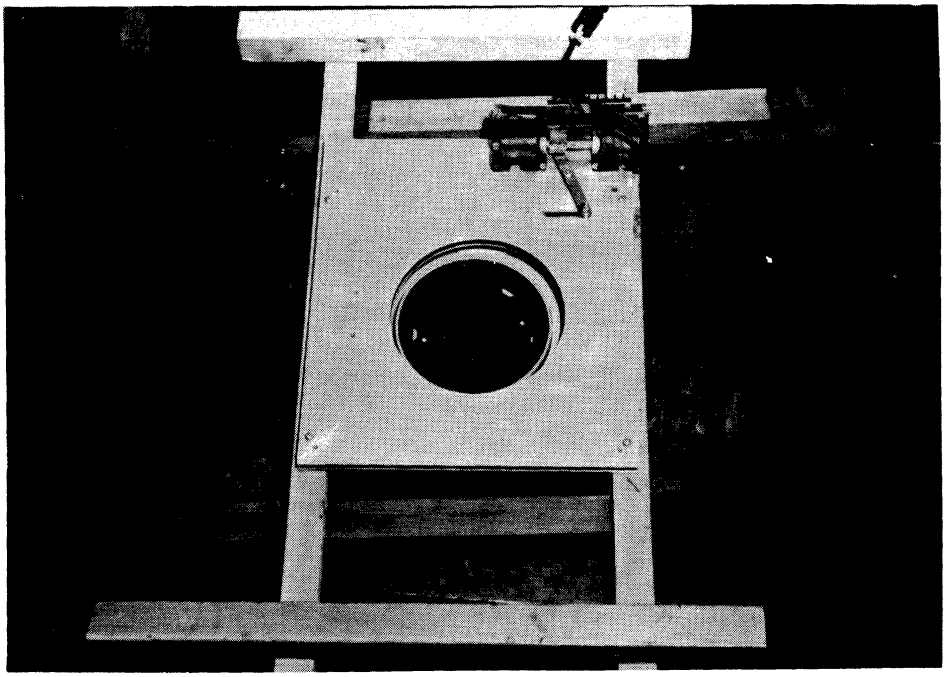

Photograph IV. This is a top view of the camera mount showing the shutter open. The solenoids that operate the shutter are illustrated. This photograph was taken through the opening in the roof.

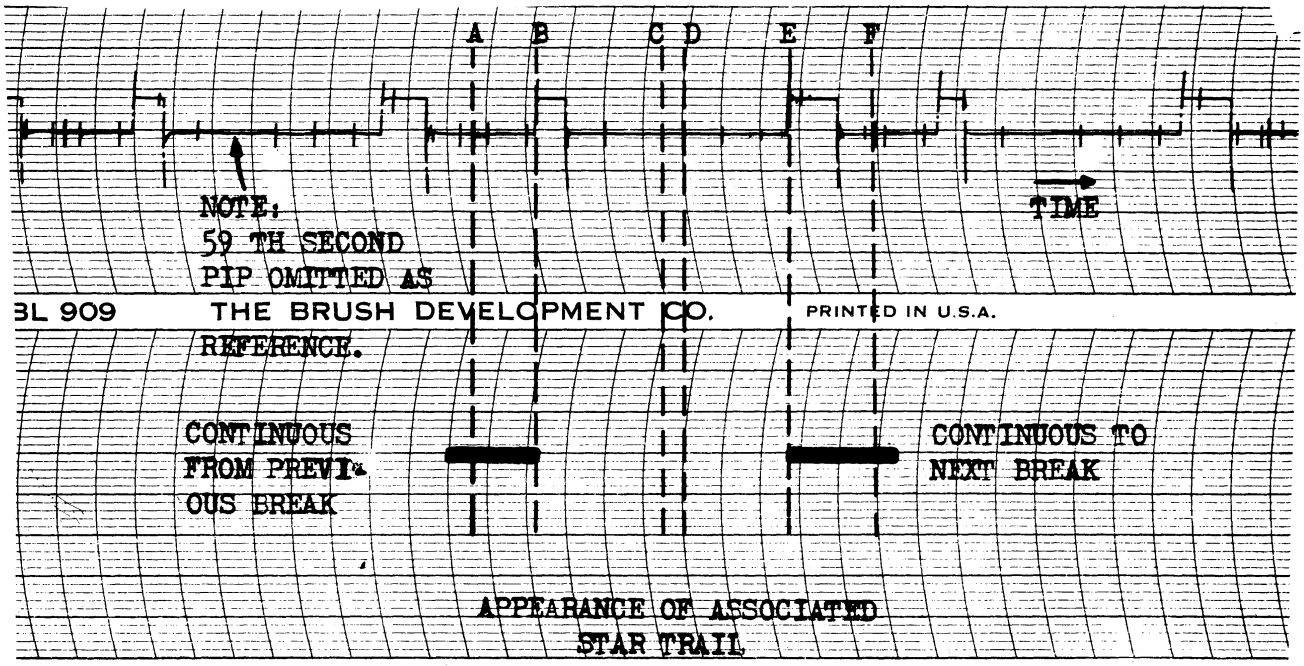

Photograph V. This illustrates the appearance of the oscillograph tape. The time sequence of events is: A, about $09^{h}47^{m}54^{s}.6$ p.m., brush oscillograph starts operating to record the break interval (cam 1); B, $09^{h}47^{m}56^{s}.3$ p.m., shutter closes starting break (cam 2); C, $09^{h}47^{m}59^{s}.5$ p.m., star at center of break; D, $09^{h}48^{m}00^{s}.0$ p.m., exact WWV time; E, $09^{h}48^{m}02^{s}.7$ p.m., shutter opens ending break (cam 3); and F, about $09^{h}48^{m}05^{s}.5$ p.m., oscillograph stops to await next trail break (cam 1). These times are found by scaling where 1 mm equals 0.2 second.

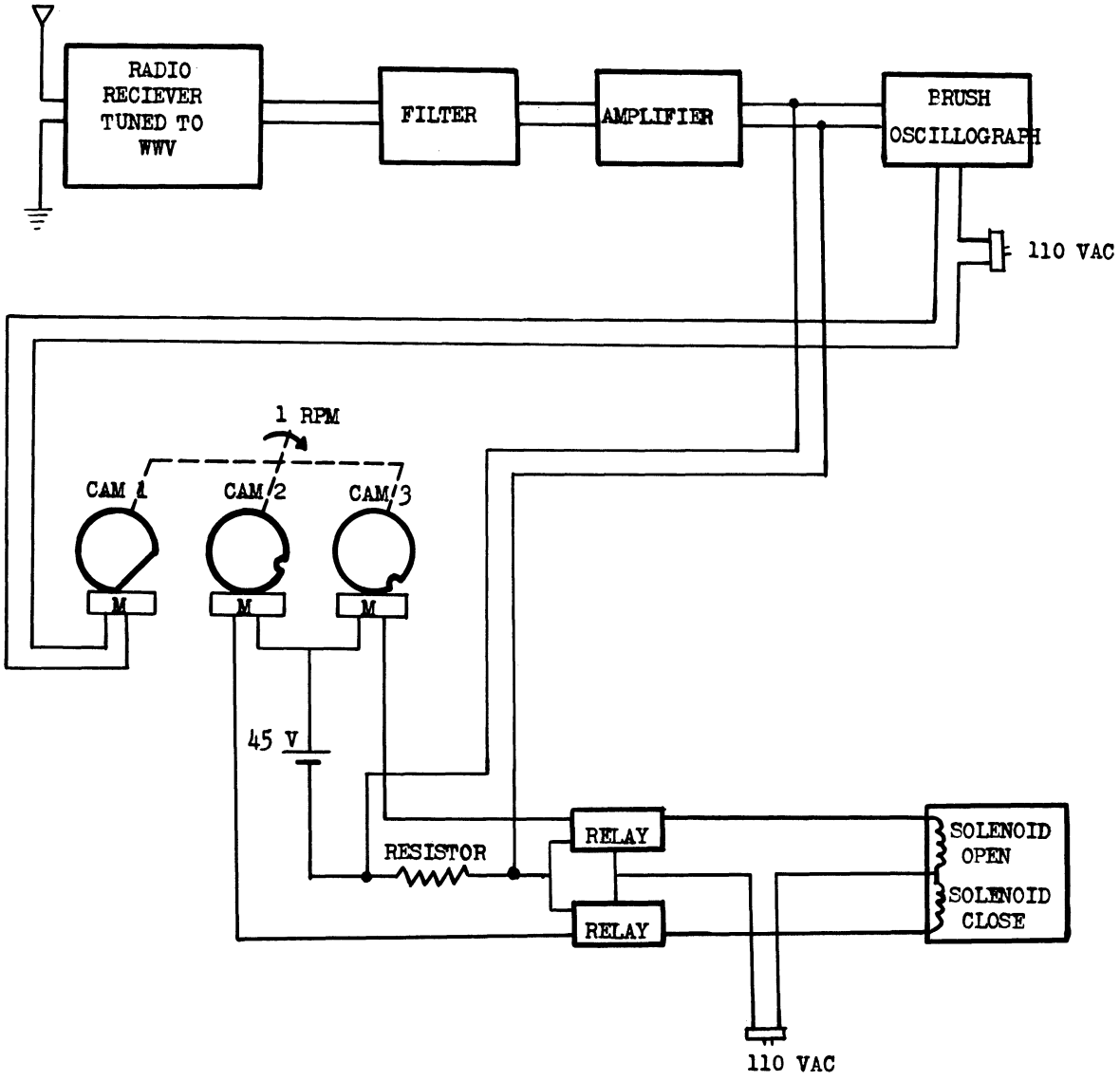
RADIO
RECIEVER
TUNED TO
WWV
FILTER
AMPLIFIER
BRUSH
OSCILLOGRAPH
110 VAC
1 RPM
CAM 1
CAM 2
CAM 3
M
M
M
45 V
RESISTOR
RELAY
RELAY
SOLENOID
OPEN
SOLENOID
CLOSE
110 VAC

Fig. 2

Filter and Amplifier Circuit

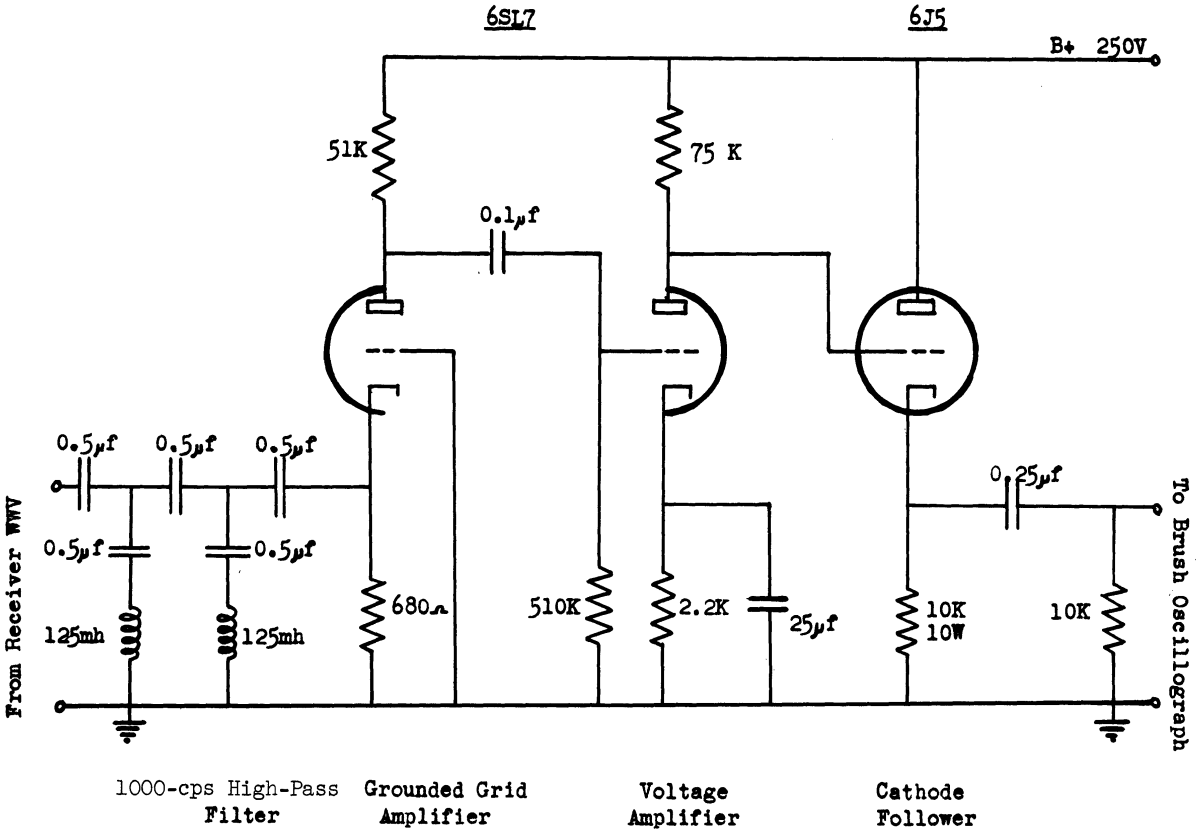

Fig. 3. A brief description of the filter amplifier circuit is as follows: Time signals from the receiver are filtered by 1000-cps high-pass filter sufficiently to remove 440-or 600-cps tone and allow the clock pulse (5 cycles of the 1000-cps note) to be recorded. The filter feeds a grounded grid amplifier which feeds another amplifier. The signal is fed to an oscillograph through the cathode follower amplifier.

REDUCTION OF STAR DATA

For most photogrammetric purposes it is desirable for the control to lie in a plane. Since we have only angular components it is preferable to project these points into some plane. The plane is selected at the astronomical zenith of the camera station and is perpendicular to the line from the camera station to the zenith. The astronomical zenith may be defined as the piercing point of the true plumb line (or gravitation vector) on the celestial sphere for a given geographic position. There are two reasons for selecting this plane. One of these will be explained in the section "Absolute Check on Tilt Determination;" the other reason lies with atmospheric refraction which is a function of the distance of a star from the zenith. The choice of this plane simplifies the calculation of this refraction.

The planar positions are obtained as follows: Consider Fig. 4 which illustrates the preceding data as well as the following reduction. The zenith distance (Z) is obtained from the following equation:

$$\cos Z = \sin \phi \sin \delta + \cos \phi \cos \delta \cos t \qquad (1)$$

where ϕ = astronomical latitude of the camera,
δ = star's declination, and
t = star's hour angle = local sidereal time* - right ascension of star.

The azimuth A is obtained from

$$\sin A = \frac{\cos \delta \sin t}{\sin Z} \qquad (2)$$

The details of these formulas are dealt with in any book on practical astronomy and will not be amplified further here. The declination and right ascension of the brighter stars are catalogued. At this project it was found that the catalogue "Apparent Places of Fundamental Stars," Her Majesty's Stationary Office, London, was sufficient. This is published annually for each year and applies to that year only.

The zenith distance computed is the actual distance and does not take into account the effect of the atmosphere. Due to refraction in the atmosphere the star image appears closer to the zenith than the computed value. The amount of this refraction can be computed knowing the temperature and barometer at the

*Local sidereal time must be computed from astronomical longitude.

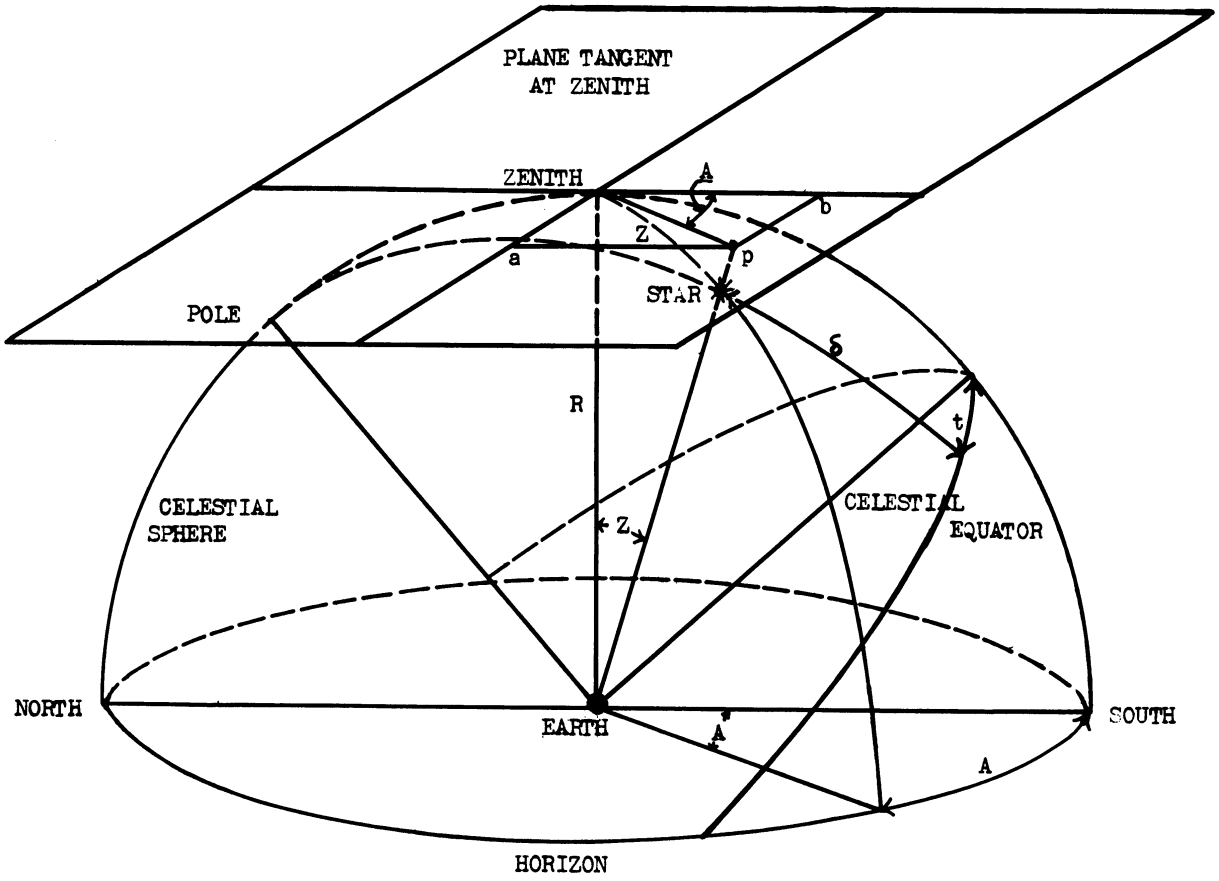

DISTANCE ap EQUALS R tan Z sin A = ξ R.

DISTANCE bp EQUALS R tan Z cos A = η R.

POINT p IS THE PROJECTION OF THE STAR ONTO THE PLANE.

Fig. 4

camera. There are several approximate formulas for finding this refraction as well as tables. A sufficient formula is

$$\Delta Z'' = \frac{983 \cdot b}{460 + T} \tan Z \qquad (3)$$

where b = barometric pressure in inches and
T = temperature Fahrenheit.

The error in this formula is less than 1 second of arc. The zenith distance as seen by the camera is then

$$Z' = Z - \Delta Z \ . \qquad (4)$$

Now the radial distance in the plane is R tan Z'. Inasmuch as R is arbitrary, it is assumed to be unity. Hence, we can find the planar position in coordinates (ξ,η) from

$$\xi = \tan Z \sin A \quad \text{and} \qquad (5)$$

$$\eta = \tan Z \cos A \ . \qquad (6)$$

These latter two equations then give the planar coordinates of the star in question with the astronomical zenith as origin and one axis the north-south line and the other the east-west line. These coordinates are called reduced coordinates. Thus, by using Equations 1 through 6 the reduced coordinates of each trail break can be computed and the entire system of angular control projected into a convenient plane.

ERROR CONSIDERATION

There are two primary sources of error in the star-trail photography method that appear in the computed reduced coordinates of the star breaks. The largest of these is due to the errors in time correlation. As noted under that topic the accuracy in time is 0.1 second. This contributes an angular position error of 1.5 seconds of arc in the extreme case. The second source of error is in the correction for atmospheric refraction. As noted this error is about 1 second of arc which contributes directly to the position error. The remaining errors are of the order of 0.1 second of arc. In view of these errors a sufficient accuracy to carry in the computations is 0.1 second in time and right ascension and 0.1 second of arc in all other angles. This simplifies the use of the star catalogues as short-term corrections can usually be neglected.

The overall error in position is about 1.8 seconds of arc and certainly less than 2 seconds of arc. With a 6-inch focal-length camera this corresponds to a maximum error on the focal plane of 0.0015 mm. From previous

investigations we have found that the combined error on the plate, due to both emulsion effects and measuring accuracy, is about 0.007 mm. Thus, the control accuracy exceeds the photographic accuracy by a factor of 5 approximately. This is more than sufficient for most photogrammetric investigations.

ABSOLUTE CHECK ON TILT DETERMINATION

The first application to be discussed is that of obtaining experimentally a check on photogrammetric tilt. This is to be done by actually measuring the tilt of the camera during exposure and then comparing the photogrammetric result with the measurement.

The photogrammetric tilt is obtained by the method of area distortion as derived in reference 5. The star-trail breaks are used as control points. Four independent solutions were worked to get a fairly strong value for tilt.

The problem of measuring the tilt is much more difficult than the photogrammetric method. Some of the difficulties are:

1. The tilt must be measured in the principal plane of the photograph or a plane parallel to it.
2. The measurement must be made without disturbing the camera to assure that the same tilt is being obtained in both cases.
3. The measuring accuracy must exceed the photogrammetric.
4. Systematic errors must be held to a minimum.

The following considerations were used in devising a method to accomplish the measurement. From previous experience we knew that the probable error in the photogrammetric tilt would probably be of the order of less than 5 seconds of arc. To exceed this value a 1-second measuring instrument would be required. To be sure that the camera is not disturbed, a method utilizing reflected light beams is preferable. Systematic errors can be reduced by measuring as directly as possible the angle between the photographic plate and the plane of control reference. The measurement can be made in the principal plane in the following manner. Disregarding the scale involved, one can consider both the photographic and the control planes to be tangent to a sphere. The two points of tangency and the lens or center of the sphere then determine the principal plane. If we had an autocollimator that turned only on an axis perpendicular to its line of sight, then the only possible position from which the autocollimator could set on both the above planes is that in which the axis is perpendicular to the principal plane. Hence, by positioning the autocollimator until it can be set on both planes the instrument can be set to turn in a plane parallel to the principal plane. To take advantage of this situation it is necessary to be able to measure the angle turned by the autocollimator to at least 1 second of arc.

EXPERIMENTAL ARRANGEMENT

Using the above considerations the following experimental arrangement was set up and used.

The Autocollimator.—The ideal instrument meeting the above conditions would be an autocollimating theodolite reading to 1 second of arc. Since we did not have such an instrument we used an ordinary theodolite equipped with an external cross-hair in front of the objective. This cross-hair is brought to the collimation axis of the telescope by adjusting its image to coincidence with the internal cross-hair in a reflecting surface. When coincidence is obtained, both direct and reversed, the external cross-hair lies on the required axis and the instrument can serve as an autocollimator. We equipped a Wild T-2 theodolite with an external cross-hair and calibrated the instrument for autocollimation to within about 2 seconds of arc.

The Reflecting Photographic and Control Planes.—The photographic plane reflecting was made by using the back surface of the photographic plate. Access to this surface is obtained by cutting a small hole in the back of the plate holder. This hole is cut in the center of the plate holder. It is masked to all but perpendicular access to hold plate fogging to a minimum. Inasmuch as the center of the plate is not needed for tilt evaluation, the fogging at the center is harmless.

The control plane was chosen at the astronomical zenith because it is then parallel to a level surface such as a liquid surface. Hence, by placing a pan of oil beneath the theodolite we have obtained a reflecting surface that is parallel to the plane of control reference.

Procedure.—Figure 5 illustrates the arrangement actually used. The procedure of the experiment follows. First, the camera is loaded and before the shutter is opened the theodolite is positioned by obtaining coincidence in both the level reflecting surface and the back of the plate. Next, the fiducial lights are flashed to record the fiducial system on the plate. The shutter mechanism is then started and we are ready to make the measurements. The theodolite is brought to coincidence on the level surface and the vernier reading recorded. This is repeated for the plate surface and then repeated again on the level surface as a check on any possible disturbance of the theodolite. These readings are then repeated with the theodolite in reversed position. The differences in the scale reading are the supplement of the tilt as measured. When the measurements have been completed by at least two observers, the mean value and probable error of the angle are obtained.

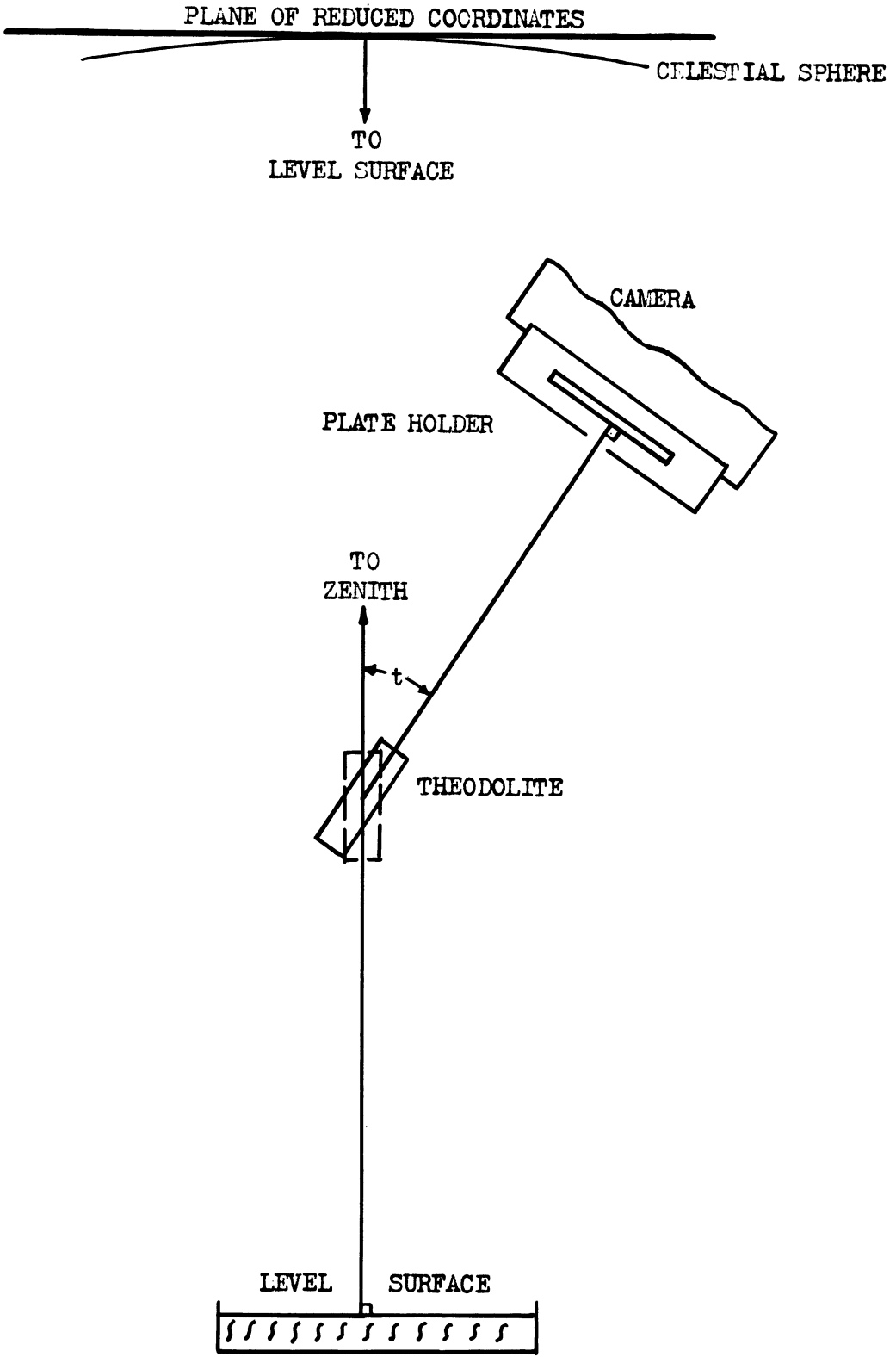
PLANE OF REDUCED COORDINATES
CELESTIAL SPHERE
TO
LEVEL SURFACE
CAMERA
PLATE HOLDER
TO
ZENITH
t
THEODOLITE
LEVEL
SURFACE

Fig. 5

ERROR CONSIDERATION

There are several sources of error in the experiment, both random and systematic. Dividing the experiment into photogrammetric tilt and measured tilt we should expect the following errors.

Photogrammetric Errors.—The major random errors in the photogrammetric procedure arise from measuring errors and random emulsion effects. From considerable experience in measuring we have found that the measuring errors are of the order of 0.005 mm. Also as a result of experiments with the glass plates used here, we find the average random emulsion displacement to be of the order of 0.005 mm. The remaining random errors arising from the residuals of systematic errors are of a lower order and do not add appreciably to the major errors. Combining these two major errors we get a mean random displacement of 0.007 mm in the plane of the photograph. The control error of 0.0015 mm does not add to this significantly. These errors should produce a corresponding average tilt error of less than 5 seconds of arc. All the above errors represent probable errors of the mean.

The systematic errors result from camera calibration, temperature effects, and emulsion creep. The first-order effects of all the above effectively change the focal length of the camera. We shall define the effective focal length to be that focal length which gives the true scale of the photograph as measured. If the effective focal length can be found, its use will eliminate the systematic errors to the first order. Of these systematic errors only emulsion creep has significant residuals and this is treated under random errors.

The effective focal length for each exposure can be found easily since in star-trail photography the "altitude" is known. By "altitude" is meant the radius of the sphere of Fig. 4. Since we made this unity the photogrammetric altitude must also be unity. The effective focal length gives the correct altitude or, in this case, one. In a given photogrammetric problem, let f_c and H_c be the calibrated focal length and corresponding altitude, respectively. Also let f_e and H_e be the effective values. Then this ratio holds approximately

$$\frac{f_e}{f_c} = \frac{H_e}{H_c} \quad . \tag{7}$$

In our case since $H_e = 1$,

$$f_e = \frac{f_c}{H_c} \quad . \tag{8}$$

By successively working the problem and applying Equation 8, f_e can be found to any accuracy desired. In practice, Equation 8 gives a sufficiently accurate value after one solution. From previous investigations we know that the error in H(ΔH) is related to the error in tilt by

$$\Delta H << H\Delta t \quad . \tag{9}$$

For H = 1 and Δt = 5 seconds of arc, we get

$$\Delta H << 2.4 \times 10^{-5} \quad . \tag{10}$$

From Equation 8, since $H_c \simeq 1$,

$$\Delta f_e \simeq f_c \Delta H \quad . \tag{11}$$

For a 6-inch lens $f_c \simeq 153$ mm and therefore,

$$\Delta f_e << 0.004 \text{ mm} \quad . \tag{12}$$

Now it can be shown that if there is an error Δf in f, the corresponding error in tilt Δt is

$$\Delta t \simeq \frac{\Delta f}{f} \times \frac{\tan t}{1 + \tan^2 t} \quad . \tag{13}$$

The tilts we are working with are about 3 degrees. Using a 6-inch lens (153 mm) and Δf from Equation 12 we get from Equation 13

$$\Delta t << 0.28 \text{ second of arc} \quad . \tag{14}$$

From this it is clear that the use of the effective focal length eliminates the first-order systematic errors from the solution for all practical purposes.

Errors in Theodolite Measurements.—In measuring, the random errors are easily dealt with as the only source in reading error with the autocollimating theodolite. We found that the probable error in this case was less than 2 seconds of arc.

The major systematic errors arise from collimation errors in the theodolite and deviations between the reflecting surfaces and their corresponding photogrammetric surfaces.

The collimation errors can be divided into errors in the plane of measurement and at right angles to that plane. Errors in the plane cancel out at once as we are taking differences from similar settings. Errors at right

angles have the effect of throwing the measurements out of the principal plane. This introduces a correction factor of the cosine of the collimation error. The theodolite was collimated to an accuracy of less than 10 seconds of arc at the most. Since the cosine of 10 seconds is unity to at least 7 digits this source of systematic error can safely be neglected.

The systematic errors from the deviations of the planar surfaces can be treated as follows. The plane of reduced coordinates and the level surface comprise one set of such surfaces. The other is the plane of the emulsion and the back surface of the photographic plate.

In the first case the error lies directly in the accuracy of determining the astronomical position of the camera. If this position were known exactly then the two surfaces would be parallel. The overall discrepancy in the position determination was about 1 second of arc. The component of this error in the principal plane is the actual error appearing in the results. As this component cannot be greater than the given error we can say that the systematic error from this source is less than 1 second of arc.

The second case arises from the fact that the photographic plates are not plane parallel. As this varies considerably from plate to plate the wedge angle must be measured in each case. The angle must then be projected into the principal plane to be able to apply a correction. The wedge angle was measured with the theodolite in much the same manner as the main measurements were made. The reading error was correspondingly the same (about 2 seconds). Since this error is random it must add to the other random error in reading. Of course, this addition must be by the law of error propagation.

The errors that contribute to the difference between photogrammetric and measured tilt can now be summarized.

Photogrammetric tilt
- Random errors, 5 seconds
- Systematic errors, negligible

Measured tilt
- Random errors, 3 seconds
- Systematic errors, 1 second

This gives a total error of 6 seconds of arc. The random errors represent the upper limits of the probable error of the mean and in practice one would expect the errors to be less than given. The total error represents the predicted difference between the two tilt determinations.

RESULTS

Four plates were used in this experiment to test the validity of the method. The final results are given below. The correction for wedge appears in the value for photogrammetric tilt.

Plate	Photogrammetric Tilt	PEM	Measured Tilt	PEM	Difference
April 8, 1954	3°-07'-06".3	5".2	3°-06'-57".3	1".2	9".0
June 22, 1954	3°-04'-13".8	3".3	3°-04'-18".4	1".5	4".6
June 23, 1954	3°-02'-14".3	2".3	3°-02'-18".0	0".3	3".7
August 3, 1954	3°-03'-49".6	3".1	3°-03'-50".5	3".4	0".9
		Avg. 3".5		Avg. 1".6	Avg. 4".6

It is of interest to note that the average errors fall well within the expected values. Also the difference is well within its predicted value. If the above figures represented a large number of trials then one could safely say that the photogrammetric tilt is true. However, due to only having four trials we will conclude that there is a good indication that photogrammetric tilt is true providing that systematic errors be removed.

NUMERICAL EXAMPLE

For a numerical example we shall take one problem from the plate of April 8, 1954, and work through the reduction to find the reduced coordinates. The standard tilt solution will be omitted along with the reduction of the theodolite readings as obvious and unnecessary.

Photograph VI illustrates the plate of April 8, 1954. Note the central fogging caused by the use of the theodolite. As can be seen this fogging is well localized and will not interfere with the experiment. The fogging at the side was caused by the moon which just started to appear on the plate. It should be noted that the moon could disrupt the experiment and should be avoided. The first break on this plate was made at 8:29 p.m. EST and the last at 11:02 p.m. EST. The average temperature during exposure was 32°F and the barometer 29.9 inches.

Breaks selected were 9-16-2-6. The measured coordinates of these breaks, corrected for lens distortion, were found to be:

Break	x (mm)	y (mm)
9	93.202	94.874
16	-64.037	82.703
2	-63.967	-76.509
6	95.248	-38.195

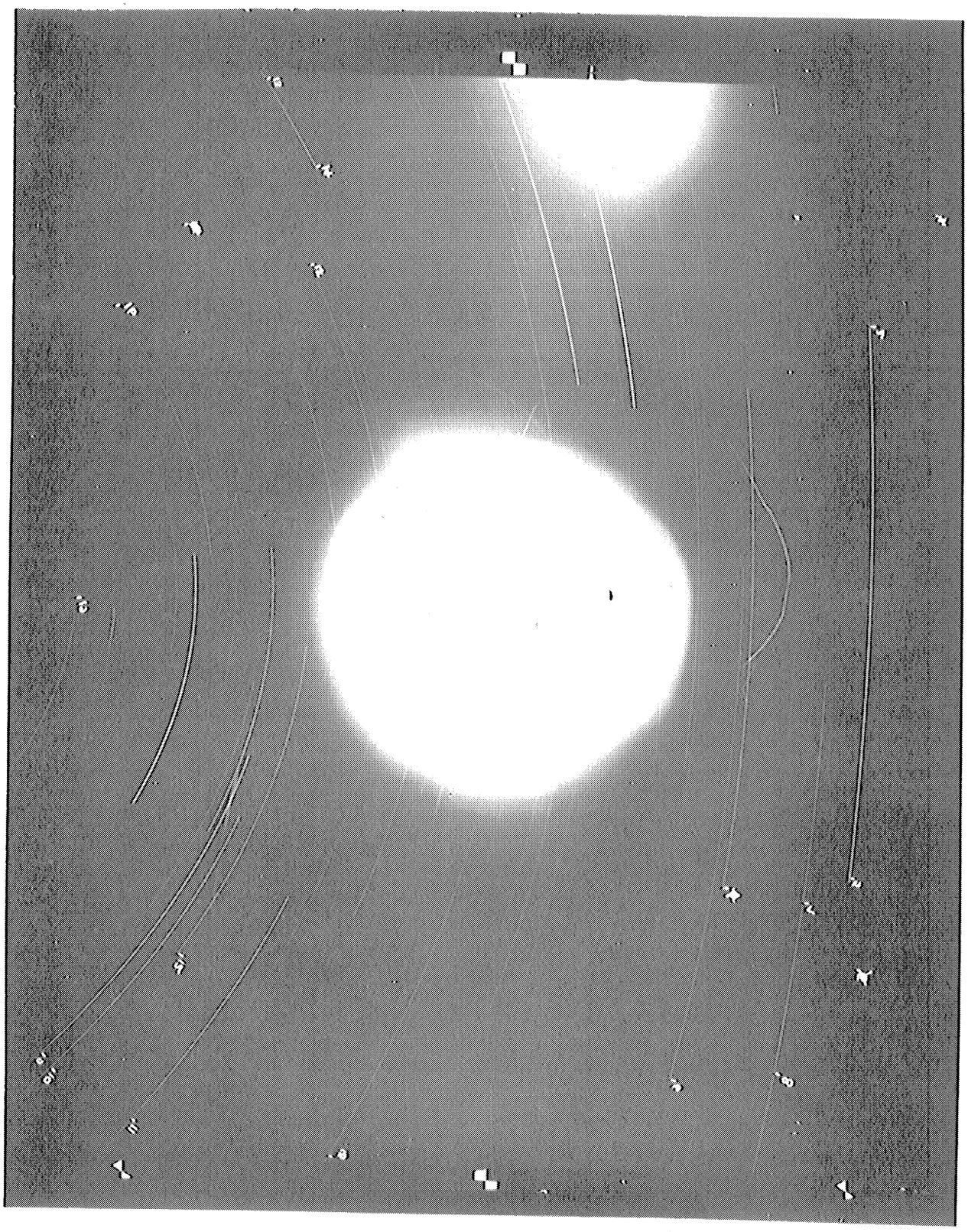

Photograph VI (Numbers were reversed, and two fiducial marks were cut off in reproduction.)

The camera was a T-11 with given focal length of 153.210 mm.

The selected stars were identified and the catalogue gave the following results for the time of the desired break:

Break	Star	Declination (δ)	Right Ascension
9	ε Ursa Major	$56^{\circ}12'18''.7$	$12^{h}52^{m}04^{s}.8$
16	o Ursa Major	$60^{\circ}52'34''.4$	$8^{h}26^{m}31^{s}.4$
2	α Leonis	$12^{\circ}11'21''.1$	$10^{h}05^{m}58^{s}.2$
6	δ Leonis	$20^{\circ}46'19''.5$	$11^{h}11^{m}42^{s}.9$

The next table gives the exact time that the star was at the center of its break, the corresponding local sidereal time, and the hour angle. At this point the astronomical longitude is needed. It has been determined to be $5^{h}34^{m}03^{s}.1$.

Break	Exact Time (EST)	Local Sidereal Time (LST)	Hour Angle (t)
9	$8^{h}30^{m}59^{s}.5$	$9^{h}04^{m}00^{s}.2$	$57^{\circ}01'09''.0$
16	$10^{h}49^{m}59^{s}.2$	$11^{h}23^{m}22^{s}.8$	$-44^{\circ}12'51''.0$
2	$11^{h}01^{m}59^{s}.0$	$11^{h}35^{m}24^{s}.6$	$-22^{\circ}21'36''.0$
6	$8^{h}28^{m}59^{s}.4$	$9^{h}01^{m}59^{s}.8$	$32^{\circ}25'46''.5$

Next we use Equation 1. For this we need astronomical latitude which is $42^{\circ}14'11''.4$. ΔZ is from Equation 3 and (ξ,η) from Equations 5 and 6. Equations 2 and 4 though applied are not listed.

Break	Cos Z	ΔZ (sec)	ξ	η
9	0.78278893	47.5	0.59577533	-0.52575539
16	0.84547659	37.7	-0.40126210	-0.48744082
2	0.81119970	43.1	-0.45819133	0.55610800
6	0.82268924	41.3	0.60920964	0.32551173

Now a tilt problem is worked using the measured and reduced coordinates. Without giving the details of the standard computation the results are

$$t = 3^{\circ}06'53''.0 \quad \text{and}$$

$$\text{"H"} = 1.000356718 \ .$$

Ratioing the focal length we find the effective focal length to be 153.155 mm. This gives in the solution

$$t = 3^{\circ}06'49''.0 \quad \text{and}$$
$$\text{"H"} = 1.000001579 \ .$$

Working the other four problems on this plate and averaging the results gives

$$t = 3^{\circ}06'54''.4 \ ,$$
$$\text{"H"} = 0.999994724 \ , \text{ and}$$
$$f_e = 153.153 \text{ mm} \ .$$

The wedge correction is 11".9 in the principal plane. Adding this gives

$$t = 3^{\circ}07'06''.3 \ .$$

The measured tilt was found to be

$$t = 3^{\circ}06'57''.3 \ .$$

This gives a final difference of 9 seconds of arc.

CAMERA CALIBRATION BY STAR TRAILS

A second and perhaps major application of star-trail photography is that of camera calibration. Such an application comes to mind immediately when one considers the accuracy with which the object space geometry is known.

CAMERA CALIBRATION

The general topic of camera calibration is well covered in the literature of photogrammetry. Some of this literature is listed in the bibliography of this report. It is not desired to do more here than summarize this topic sufficiently to give an adequate background for this specific application.

An ideal lens system would reproduce an object space in its focal plane with an exact angular reproduction. If the focal length were known the scale would also be known. A real lens system fails to meet this condition. The purpose of calibration is to find the deviations in the angular field and to find the corresponding focal length. Thus, when a camera has been calibrated

it should be possible to take a given photographic image and compute the undeviated position of that image on the photograph as well as to compute the scale of the object space. The calibration must be tied to the fiducial axes of the camera to do this.

Photogrammetric lens systems are designed symmetrically to the central axis of that system. For this reason it is assumed that the angular distortions in the field are also symmetric to that axis and radial to it. Actually, there are also asymmetrical effects caused by decentering of lens elements and sometimes wedges in the form of filters, pressure plates, etc; these produce asymmetrical distortions. For most lens systems the radial component of distortion is much larger than the tangential or remaining elements. The calibration to be discussed prescribes that all distortions exhibit some form of central symmetry or are translational. Any remaining distortions will be assumed to be small of the order of measuring accuracy and residual emulsion creep. This assumption is valid for the modern mapping camera. It might be mentioned that the method to be used can be adapted to calibrations where symmetry cannot be found. Here we shall restrict the discussion to symmetry.

The method to be given is applied to the metrogon lens. The modification to other lens systems with different characteristic distortion patterns should be apparent. The metrogon lens exhibits the two symmetries illustrated in Fig. 6. These distortions are characteristic of this type of lens.

The focal length of a lens system is actually quite difficult to find. The reason for this lies with the distortions. The focal length is found by scaling between the image and the object space. Since the images are displaced according to their positions on the photograph, the lens system actually has a range of focal lengths. This difficulty is overcome by finding a focal length that gives a specific distortion at a given position on the photograph. This focal length is called the calibrated focal length and has significance only if the method of selection is given along with the corresponding distortion.

There is another point that should be discussed. In order to use the distortions as illustrated in Fig. 6, it is necessary to know about what point on the photograph these distortions are symmetric. This point is called the point of symmetry.

There are in addition to the point of symmetry two other points in calibration theory. One of these is the foot of the plate perpendicular from the lens node and the other the trace of the central ray on the photograph. We propose to add the calibrated principal point of reference 1. The calibrated principal point is that point about which some prescribed symmetry or asymmetry exists. Since we are prescribing symmetry the calibrated principal point and the point of symmetry coincide in our case. If we prescribed asymmetry these points would not coincide. The foot of the plate perpendicular has theoretical significance only since there is no true nodal point in a real lens

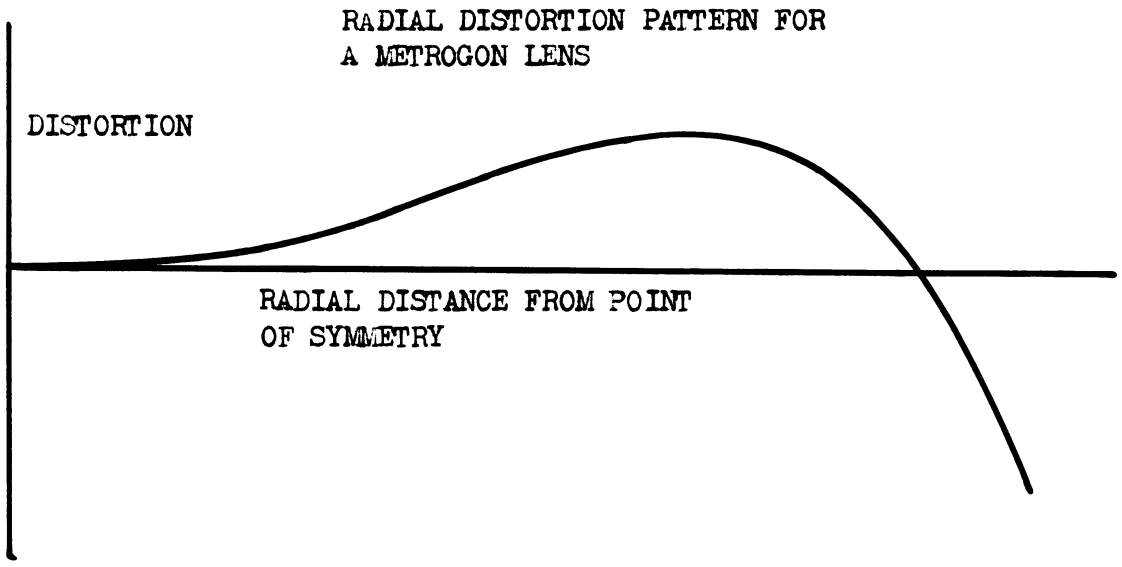
RADIAL DISTORTION PATTERN FOR
A METROGON LENS
DISTORTION
RADIAL DISTANCE FROM POINT
OF SYMMETRY

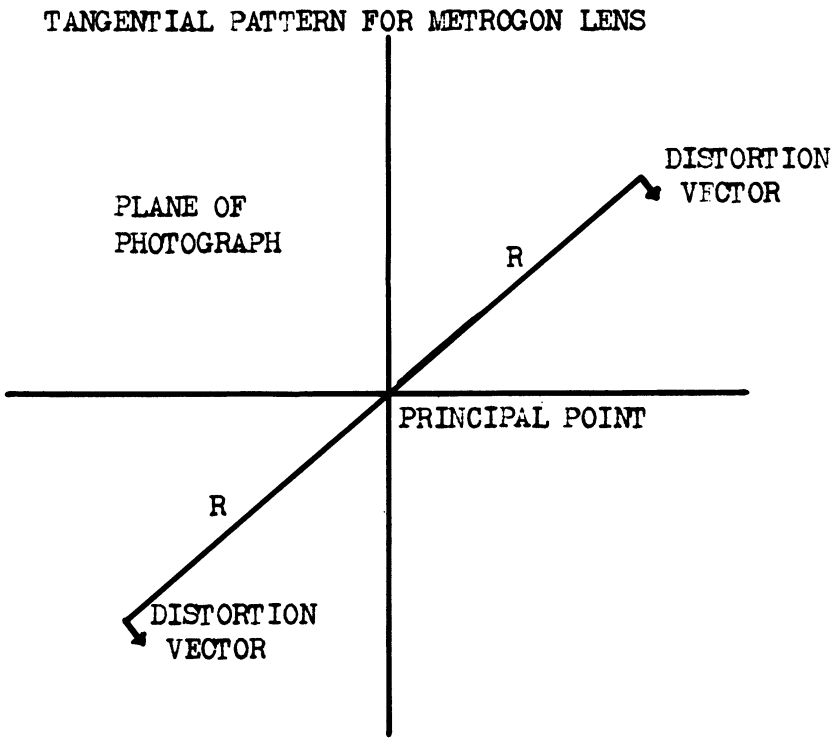
TANGENTIAL PATTERN FOR METROGON LENS
PLANE OF
PHOTOGRAPH
DISTORTION
VECTOR
R
PRINCIPAL POINT
R
DISTORTION
VECTOR

Fig. 6

system. In the reduction it will be apparent that the calibrated principal point serves effectively as this point. The trace of the central ray has no significance in the calibration to be carried out.

Thus, the lens system can be considered calibrated if the calibrated focal length, the distortions, and the point of symmetry are given. There remains only the problem of relating the calibration to the camera as a whole. This is done through the fiducial marks which are fixed in the camera with respect to the lens. The connection is established by finding the position of the point of symmetry with respect to the fiducial marks. It is also customary to measure the perpendicularity of the fiducial axes and the distance between the ratioing markers.

From the foregoing it can be seen that there is an infinite number of calibrations that can be made by varying the prescribed distortions in both symmetry and magnitude. All are equivalent in the sense that from the calibration the object geometry can be restored. The use of the point of symmetry permits the calibration to be expressed in its most compact form and is therefore preferable. The calibration to be made prescribes the symmetries of Fig. 6 and the calibrated focal length is chosen to make the maximum radial distortion equal to that of the manufacturer's calibration.

FIELD CALIBRATION

The object of field calibration is to avoid the use of elaborate equipment in doing the calibration. The method of star-trail calibration requires only the use of the equipment referred to previously in order to produce the star trails with time correlation. The camera for this purpose need not be located at an exactly surveyed point. The approximate or map position of the camera is sufficient for this purpose. The camera need only to be mounted rigidly with a clear view of the sky. One exposure of sufficient length to cover the photograph adequately is enough for the entire calibration. As in most field-type calibrations the lack of equipment is made up by the necessity of more elaborate data reduction procedures. However, if one wished to employ such a method for the calibration of cameras on a large scale, these reductions could be programed for automatic computation.

DATA REDUCTION

In general this method will be to superimpose mathematically the object space on the image space with suitable scale and to adjust this object space until the differences in position of corresponding points attain the desired or prescribed conditions. Then the superimposed position of the object origin will be the point of symmetry and the scale will give the calibrated focal length. This is possible with star-trail photography as the nature of

the object space permits transformations that do not alter its angular positions.

This procedure is done in two steps. Step one is to make the large-scale adjustment so that the remaining corrections can be made on a differential scale. Step two is to make the final adjustment to meet the prescribed calibration conditions. The latter adjustment is made in a manner very similar to the method of R. Roelofs in reference 1.

Step one is made as follows. Consider Fig. 7 which shows only two dimensions for simplicity. The object positions have been found in the plane tangent at the approximate zenith. The photographic positions have been measured with respect to the fiducial axes.

Before proceeding, the only reason for using the approximate zenith plane is to make the refraction corrections. From Equation 3 it can be seen that Z could vary by 2 or 3 minutes without changing ΔZ at all to three digits. Since ΔZ has only three digits for any practical zenith distances Z and also the zenith itself need only be known to 2 or 3 minutes. For this reason the camera position need only be known within 2 or 3 minutes corresponding to about 2 or 3 miles on the surface of the earth.

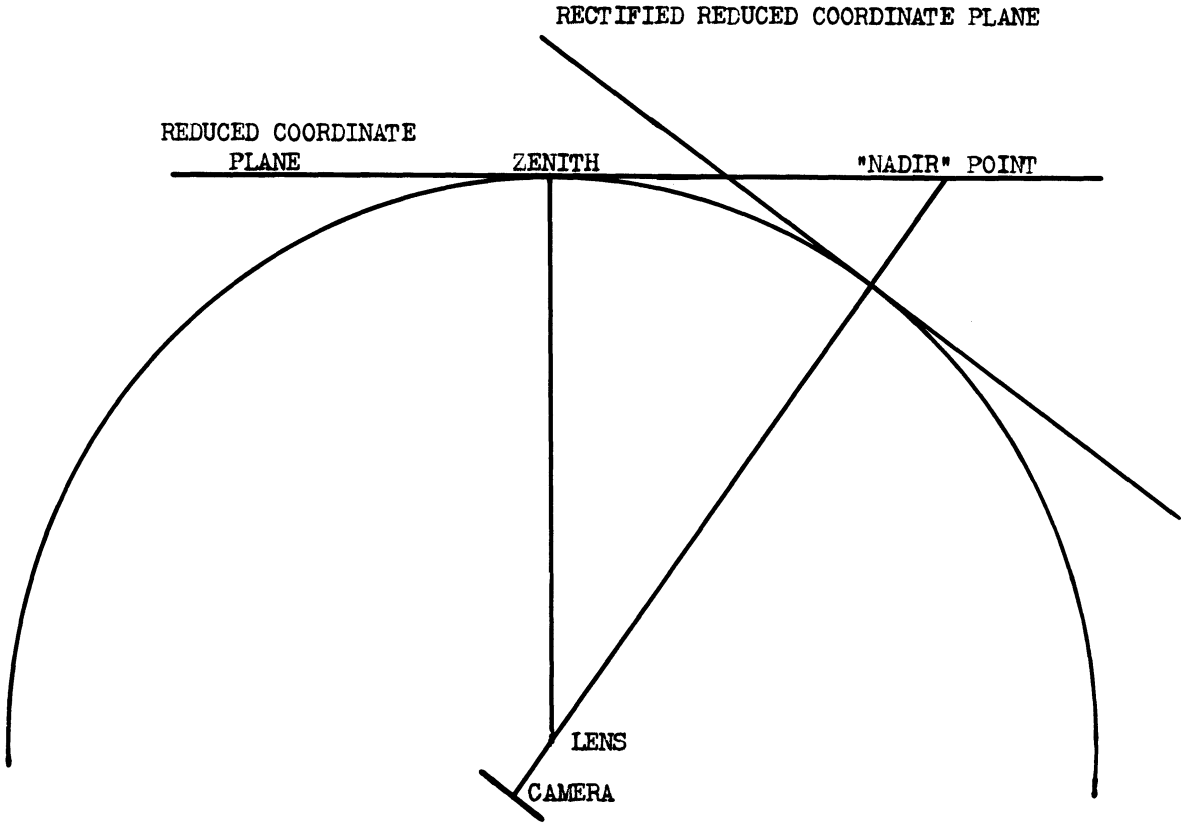

Fig. 7

Now we reverse the concept of image and object space and consider the reduced coordinates the "camera system" with focal length unity. The photographic coordinates are in similar manner considered as the control. With these data we can find the tilt and the "nadir" point in the reduced coordinate system. This is done by selecting four or five strong tilt problems and taking the mean of the solutions. The result is only approximate because the distortions are still in the solutions. The reduced coordinate system is then rectified to the new "nadir" point by the rectification transformation of reference 4. From Fig. 7 it can be seen that this brings the reduced coordinate plane to approximate opposition to the photographic plane. This removes the large-scale tilt distortion between the two systems of coordinates (photographic and reduced). The transformation is

$$\xi' = \frac{\xi \dfrac{\eta_n^2 S + \xi_n^2}{\xi_n^2 + \eta_n^2} + \eta \dfrac{\xi_n \eta_n (1-S)}{\xi_n^2 + \eta_n^2} - \xi_n}{\xi_n \xi + \eta_n \eta + 1} \quad \text{and} \tag{15}$$

$$\eta' = \frac{\eta \dfrac{\xi_n^2 S + \eta_n^2}{\xi_n^2 + \eta_n^2} + \xi \dfrac{\xi_n \eta_n (1-S)}{\xi_n^2 + \eta_n^2} - \eta_n}{\xi_n \xi + \eta_n \eta + 1} \tag{16}$$

where $S = (\xi_n^2 + \eta_n^2 + 1)^{1/2}$,

(ξ_n, η_n) = reduced coordinate nadir point,

(ξ, η) = reduced coordinate field point,

(ξ', η') = transformed field point in new plane.

We know from experience with the tilt solution that error in tilt introduced by the distortions is probably no more than 2 or 3 minutes of arc. This small remaining tilt can certainly be dealt with on a differential scale.

Differences still remain between the (ξ', η') and (x,y) systems consisting of scale, rotation, and translation. Here (x,y) indicates the photographic coordinate system. These are removed by selecting a group of points near the center of the photograph where distortion is negligible and solving Equations 17 and 18 by least squares for the rotation (θ), the scale (f), and the translation $(\Delta x, \Delta y)$:

$$x = \xi' f \cos\theta + \eta' f \sin\theta - \Delta x \quad \text{and} \tag{17}$$

$$y = \eta' f \cos\theta - \xi' f \sin\theta - \Delta y \ . \tag{18}$$

These equations are then applied to the (ξ',η') system giving the object space coordinates (x',y'). This completes step one. Since f, θ, Δx, and Δy were computed from points with negligible distortion, these values should be very close to the correct values. We now have the desired condition that the two systems of coordinates (x',y') and (x,y) differ by very small amounts. The differences between corresponding points are the distortions. These distortions are put in the form of radial (D_r) and tangential (D_t) distortions and inspected for symmetry. As symmetry here would only be accidental it will probably be necessary to make further adjustments of the prime system to attain symmetry. These adjustments are given in the second step.

Step two is made as follows. First, the residual tilt is removed to attain the desired symmetry. The first-order expression for Equations 15 and 16 with scale f become

$$x' = x - dx - \frac{x^2}{f^2}\,dx - \frac{xy}{f^2}\,dy \quad \text{and} \tag{19}$$

$$y' = y - dy - \frac{y^2}{f^2}\,dy - \frac{xy}{f^2}\,dx \quad . \tag{20}$$

Note that these expressions contain translations dx and dy. We do not wish this type of rectification as the origins have already been superimposed by Equations 17 and 18. Physically the geometry with respect to tilt is shown in Fig. 8. The transformation here is minus the translation or

$$x' = x - \frac{x^2}{f^2}\,dx - \frac{xy}{f^2}\,dy \quad \text{and} \tag{21}$$

$$y' = y - \frac{y^2}{f^2}\,dy - \frac{xy}{f^2}\,dx \quad . \tag{22}$$

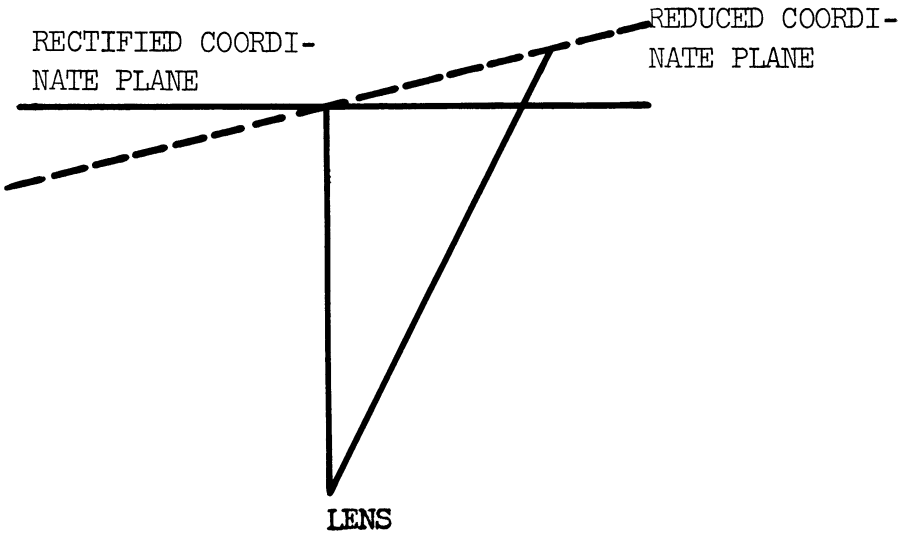

Fig. 8

The method of applying these equations may vary according to available control points and varying prescribed distortions. In this case we took symmetrically opposite points and set up Equations 21 and 22 to make the radial and tangential distortions equal in the sense of Fig. 6. The method of doing this is to find ΔD_r and ΔD_t as introduced by Equations 21 and 22 for each point. These expressions will be linear in dx and dy. By equating these expressions for equality in distortions for symmetrically opposed points we will get two linear equations in dx and dy for each set of points. By selecting several pairs of such points a least squares solution is possible for dx and dy. If symmetry is obtained after applying Equations 21 and 22 to the (x',y') system, we have found the corrections. If not, the solution can be repeated on the assumption that the correction is too large for differential solution. If symmetry exists a sufficient number of solutions will converge to the correct results. If symmetry does not exist then the prescribed distortions must be altered to meet the physical situation. In almost every case if symmetry exists the first solution will be sufficient. The corrections dx/f and dy/f should be added to ξ_n and η_n, respectively, as they represent the tilt corrections; it is equivalent to add them to Δx and Δy. Therefore, the coordinates of the point of symmetry become

$$\Delta x + dx \quad \text{and} \tag{23}$$

$$\Delta y + dy \quad . \tag{24}$$

Next the correction to f is found by making the magnitude of radial distortion meet the prescribed conditions. This is easily done as the radial distortion at a lens angle α is changed by $\Delta f \tan \alpha$ for a change Δf in f. The calibrated focal length is then

$$f + \Delta f \quad . \tag{25}$$

Finally, the angle θ is corrected so that no residual rotation remains in the distortions. This is done by finding a $\Delta\theta$ such that the sum of all rotations produced by tangential distortion is zero. Then each tangential distortion is corrected by $r\Delta\theta$ where r is the radial distance of the point in question.

The values from Equations 23, 24, and 25 together with the finally computed distortions are the calibration constants and step two is completed.

The measuring of the distance between ratioing markers and the orthogonality of the fiducial axes is standard and will not be discussed here.

NUMERICAL EXAMPLE

To explain the foregoing reductions further, a numerical example will be given. This example is only complete enough to explain the reductions. Consider Photograph VII which illustrates the star-trail plate of June 1-2, 1953. Four lines of breaks were selected on this plate to determine the distortions. In addition, the eight numbered breaks were selected for the purpose of solving Equations 17 and 18. These breaks, which we shall refer to as the central breaks, lie approximately on a circle with approximate radius of f tan 10 degrees. The other breaks are identified by numbering them from the letter identifying the line. We shall select two symmetric pairs of points on each diagonal line and follow the reductions with them. The points selected are d-2, d-14, b-4, and b-12. Only one of the central group will be followed as sufficient. Point 1 will be used for this. The solutions given however will be from the entire system.

The reduced and measured coordinates are given data.

	Measured Coordinates		Reduced Coordinates	
Break	x (mm)	y (mm)	ξ	η
1	-0.124	26.888	0.0048419	0.1779866
b-4	-79.331	65.470	-0.5044412	0.4449614
b-12	63.794	-78.712	0.4005169	-0.5222641
d-2	-85.010	-97.815	-0.5718617	-0.6179102
d-14	78.220	103.280	0.5315709	0.6620271

We are ready to start step one at once. Five tilt problems were selected and worked. The mean result was found to be

$$\xi_n = 0.000147907 \quad \text{and}$$

$$\eta_n = 0.002608095 \ .$$

Substituting in Equations 15 and 16 the transformation becomes

$$\xi' = \frac{1.000003401^{\xi} - 0.000000193^{\eta} - 0.000147907}{0.000147907^{\xi} + 0.002608095^{\eta} + 1} \quad \text{and}$$

$$\eta' = \frac{1.000000011^{\eta} - 0.000000193^{\xi} - 0.002608095}{0.000147907^{\xi} + 0.002608095^{\eta} + 1} \ .$$

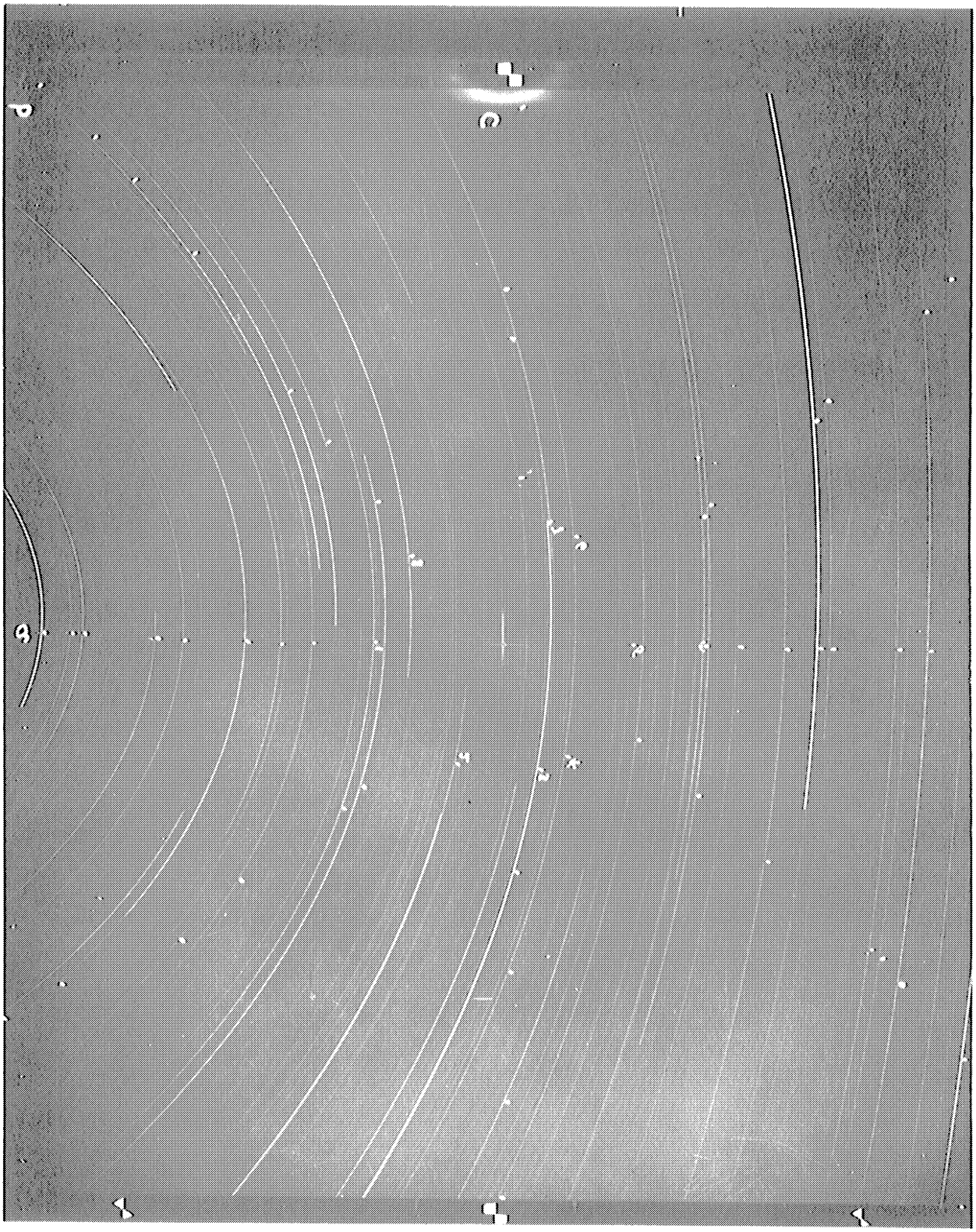

Photograph VII (Numbers were reversed, and two fiducial marks were cut off in reproduction.)

All the points are now transformed to the new plane.

	New Reduced Coordinates	
Break	ξ'	η'
1	0.004691794	0.175297007
b-4	-0.504043572	0.441873581
b-12	0.400892769	-0.525557013
d-2	-0.572983298	-0.621572472
d-14	0.530467046	0.658230637

Next, Equations 17 and 18 are formed from the central breaks from break 1.

$$-0.124 = 0.004691794\, f \cos\theta + 0.175297007\, f \sin\theta + \Delta x + 0\Delta y \quad \text{and}$$

$$26.888 = 0.175297007\, f \cos\theta - 0.004691794\, f \sin\theta + 0\Delta x + \Delta y \ .$$

From the eight central breaks we get sixteen such equations. Solving them by least squares we get

$$\sin\theta = -0.029720872 \ ,$$

$$f = 153.1681528 \text{ mm} \ ,$$

$$\Delta x = -0.0394612 \ , \text{ and}$$

$$\Delta y = 0.027052 \ .$$

The (ξ', η') coordinates are now substituted in the equations giving

Break	x'	y'
b-4	-79.220	65.384
b-12	63.730	-78.611
d-2	-84.934	-97.744
d-14	78.179	103.217

The coordinate components of the distortion are now x-x' and y-y'. These coordinates are projected on the radial line and perpendicular to the radial line to find D_r and D_t, respectively. By definition we will call D_r positive toward the center and D_t positive for clockwise rotation. This is regarding the distortion as going from x to x' and y to y'. The results are:

Break	(x-x') mm	(y-y') mm	D_r (mm)	D_t (mm)
b-4	0.111	0.086	0.140	0.005
b-12	0.064	0.101	0.119	-0.014
d-2	0.076	0.071	0.103	-0.011
d-14	0.041	0.063	0.075	0.006

It is apparent from this that symmetry has not been attained. Therefore, we proceed with step two. It was found on inspecting the results from all the breaks on this plate that the tangential distortions were very low. The percentage error in these distortions was so high that it was felt that they would not contribute usefully to the next step in the reduction. Therefore, only the radial distortions were used in the next step.

Equations 21 and 22 become

Break			
b-4	$\Delta x'$	=	-0.2675 dx +0.2208 dy
	$\Delta y'$	=	0.2208 dx -0.1822 dy
b-12	$\Delta x'$	=	0.1731 dx +0.2135 dy
	$\Delta y'$	=	0.2135 dx -0.2634 dy
d-2	$\Delta x'$	=	-0.3075 dx -0.3539 dy
	$\Delta y'$	=	-0.3539 dx -0.4072 dy
d-14	$\Delta x'$	=	-0.2605 dx -0.3440 dy
	$\Delta y'$	-	-0.3440 dx -0.4541 dy

Now projecting these corrections onto the radial line and taking the proper sign convention into consideration, we get the following corrections to the radial distortions.

Break			
b-4	ΔD_r	=	-0.3468 dx +0.2863 dy
b-12	ΔD_r	=	0.2748 dx -0.3391 dy
d-2	ΔD_r	=	-0.4688 dx -0.5395 dy
d-14	ΔD_r	=	0.4315 dx +0.5697 dy

The condition that the radial distortions be equal for symmetric points gives for two such points a and b

$$D_{r_a} + \Delta D_{r_a} = D_{r_b} + \Delta D_{r_b} \quad .$$

From the known values this gives

b-4 and b-12 $\quad -0.6216\ dx + 0.6254\ dy = -0.021$ and

d-2 and d-14 $\quad -0.9003\ dx - 1.1092\ dy = -0.028$.

The solution to a large number of such points gives by least squares

$$dx = 0.025 \quad \text{and}$$

$$dy = 0.002 \ .$$

Equations 23 and 24 give for the point of symmetry

$$x = -0.014 \quad \text{and}$$

$$y = 0.029 \ .$$

Making the distortion equal to the maximum distortion of the manufacturers gives $\Delta f = -0.006$ mm. Equation 25 gives for the calibrated focal length f_c

$$f_c = 153.162 \text{ mm} \ .$$

TEMPERATURE EFFECTS

The major difficulty with field calibration arises from the fact that the calibrations are not made at a uniform temperature. Since the exact dimensions of the camera system are a function of temperature, the computed focal length is also affected by the same function of temperature. If this function together with the temperature is known, the focal length can be found for some standard calibration temperature. For practical purposes we may regard the function

$$F(t) = 1 + k(T_1 - T_2) \tag{26}$$

to express the ratios of corresponding dimensions at temperatures T_1 and T_2. In terms of the focal length f Equation 26 can be expressed

$$\Delta f = K(T_1 - T_2) \tag{27}$$

where $K = fk$.

The temperature effects to be considered are (1) expansions of the glass plate between exposure and measurement and (2) expansions in the lens-cone combination of the camera.

Since we have not been able to obtain the temperature coefficients from the manufacturer at this time we will assume typical values. For f equals 153 mm, Equation 27 gives

$$\text{for glass,} \qquad \Delta f = 0.000757 \text{ mm/T} = K_1 \ .$$

The T-5 camera has an aluminum cone giving

$$\text{for aluminum,} \qquad \Delta f = 0.001559 \text{ mm/T} = K_2 \ .$$

In each case the measuring temperature was higher than the exposure temperature. For this reason the computed focal length is larger than that of exposure. Using 72 degrees for the standard temperature of calibration we have by combining the two effects

$$f_{72} = f_c + K_1(T_{ex} - T_m) + K_2(72 - T_{ex}) \qquad (28)$$

where f_{72} is the focal length ratioed to 72 degrees,
f_c is the computed focal length,
T_{ex} is the exposure temperature, and
T_m is the measuring temperature.

RESULTS

Since the error considerations are too complex for theoretical investigation, we can best find the errors by repeating the calibration several times and comparing results. With this in mind the calibration was repeated four times. The temperature correction for focal length is given by Equation 28. A similar equation for any distance D is found by multiplying Equation 28 by D/f or D/153. The distances and orientation of the plate are given in Fig. 9.

The manufacturer's calibration is

Camera	T-11 Serial No. 51-193
Cone	Serial No. SF220
Lens	Serial No. SF220
Cal. f (72°)	153.210 mm
A-B (72°)	237.07 mm
C-D (72°)	235.39 mm
Ratioing markers	153.210 ± 0.05 mm
Angle A	90° ± 1'
Point sym	(0.007,0.010) mm

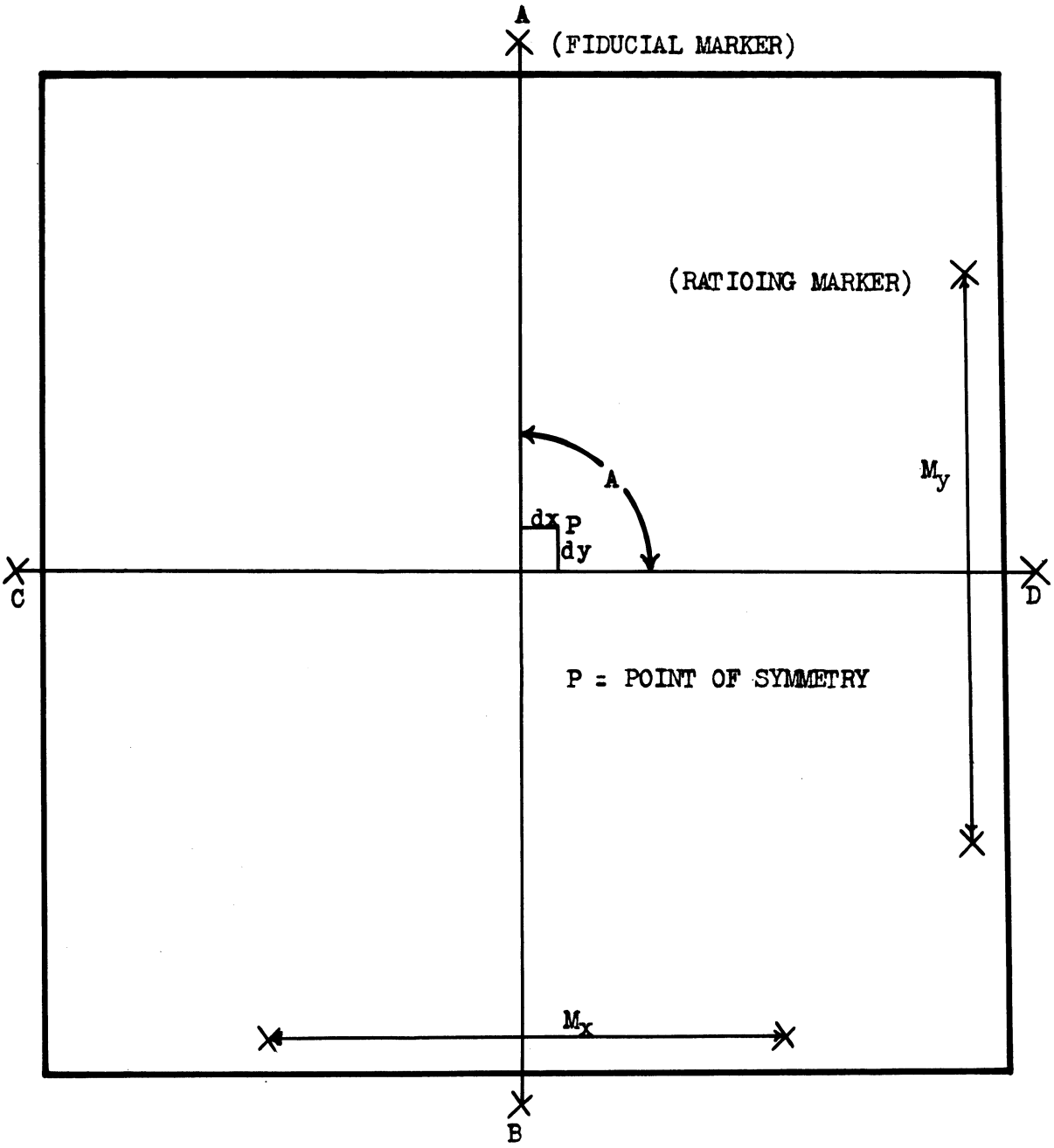

EMULSION UP

Fig. 9

Our results for the same data are

Plate	$f_c(72°)$mm	(dx,dy)mm	A(90°+)	A-B(mm)	C-D(mm)	M_x(mm)	M_y(mm)
1	153.181	-0.011,0.024	7.4	237.071	235.390	153.219	153.192
2	153.180	-0.016,0.009	-0.4	237.092	235.406	153.229	153.206
3	153.175	-0.014,0.029	-20.7	237.080	235.424	153.232	153.205
4	153.173	-0.004,0.012	-29.9	237.094	235.375	153.218	153.206
Avg.	153.177	-0.011,0.019	-10.9	237.084	235.399	153.225	153.202
P.E.	0.002	0.004,0.006	12	0.007	0.014	0.005	0.005

The most significant thing to notice from the results is the probable error for it gives a representative value for accuracy. The actual values for distances unfortunately cannot be properly compared as our temperature coefficients were only typical values for the material used; however, dx and dy are unaffected by temperature due to their magnitudes. Also the angle A is unaffected by temperature. The angle A is in good agreement with the original specifications. Since the calibration certificate didn't give errors for dx and dy, we can only assume that they are at least as large as ours and hence the two error ranges overlap giving agreement. The condition of 0.05 mm on the ratioing markers in the certificate does not permit comparison.

It is still possible to compare f_c, A-B, and C-D even without temperature coefficients. Our A-B and C-D average larger than the certificate's by about 0.011 mm. It is then reasonable to argue that our f_c is also larger since the effects of temperature are uniform. Actually our f_c is smaller by 0.033 mm. Since both values were selected to give the same distortions this indicates that the f_c's are not in agreement.

The radial distortions obtained are illustrated in Fig. 10. This is a composite curve for all four plates. It is possible to estimate the probable error in this curve from its width. A reasonable estimate is 1/3 of the width. This is about 7 or 8 microns. It is important to notice that 7 microns is the average position error due to measuring and emulsion errors. This is an indication that this method of calibration is at least equal in accuracy to the limits imposed by the emulsion and measuring accuracies. No calibration procedure can hope to exceed these limits.

For tangential distortion we found that almost all the points were within the error limits of 7 microns. We are unable to find a significant pattern and must conclude that this lens has negligible tangential distortion. This is very unfortunate for our purposes since the method was devised with the purpose in mind of finding the tangential distortion pattern along with the radial pattern from one exposure. It would be very interesting to try this method on a decentered lens system where the tangential distortion is large.

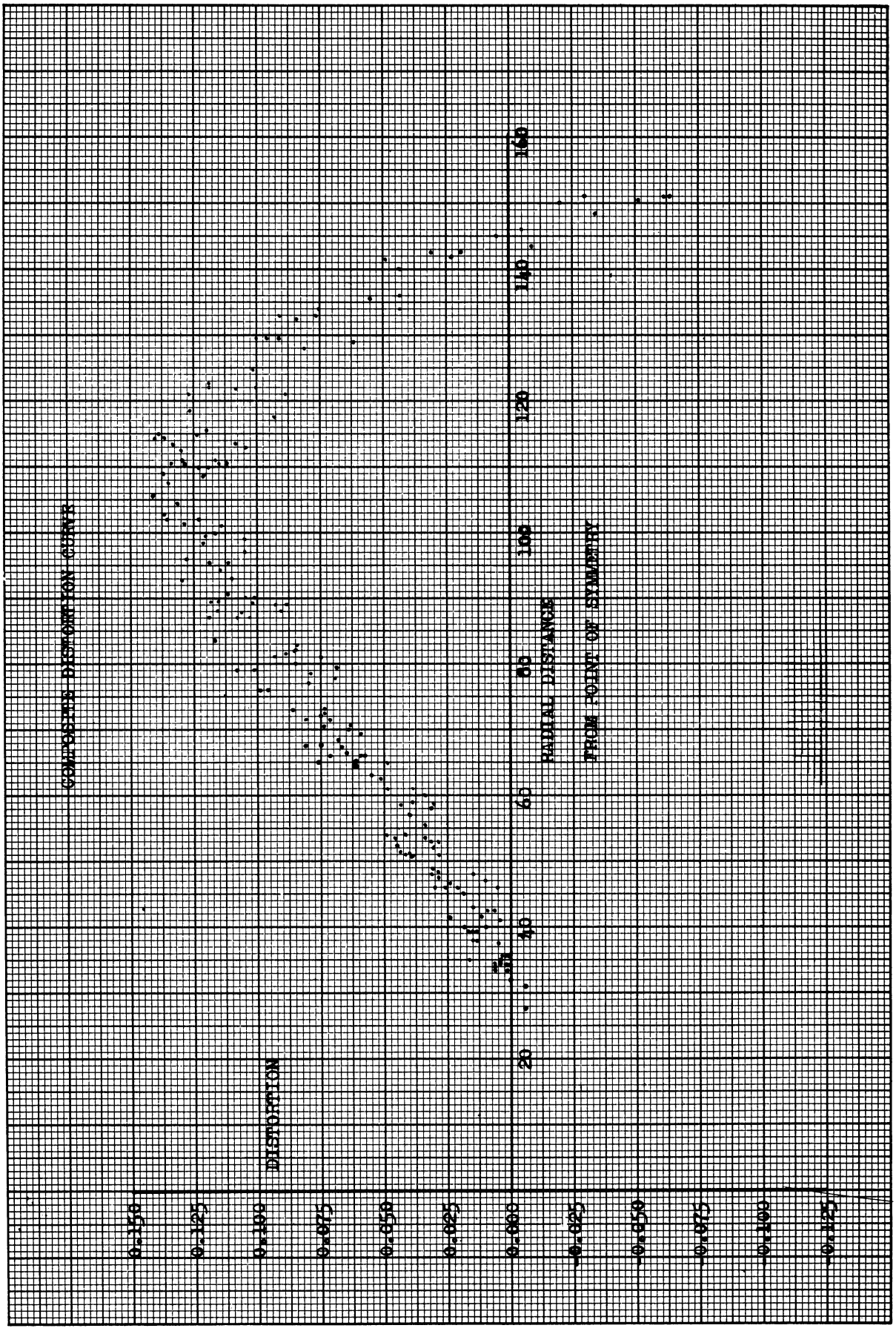
CONFOCAL DISTORTION CURVE
RADIAL DISTANCE
FROM FOCUS OF SYMMETRY
DISTORTION
160
140
120
100
80
60
40
20
-0.150
-0.125
-0.100
-0.075
-0.050
-0.025
0.000
0.025
0.050
0.075
0.100
0.125

Fig. 10

We can conclude from this experiment that one can expect the following accuracies from this type of calibration:

Component	Approximate Accuracy (P.E.)
Distortion	0.007 mm
f_c	0.002 mm
Point of symmetry in coordinates	0.005 mm
Angle between axes	12 sec
Ratioing distances	0.007 mm

CONCLUSIONS

The two most significant advantages of star-trail photography are:

1. Star trails represent the most ideal control system from the point of view of photography.
2. The control system can be adapted easily to any location and be arbitrarily oriented to any position desired. This can be done with no loss in accuracy.

The two examples demonstrated how such a control system can be utilized in photogrametric applications where accuracy is the paramount objective.

Photogrammetrists have been using star photography for some time as can be seen in the bibliography. It is hoped that this report will increase the general knowledge in this field. The method in calibration used here could be adapted to practical calibration procedure when the indicated accuracy is desired.

BIBLIOGRAPHY

1. Roelofs, R., "Distortion, Principal Point, Point of Symmetry, and Calibrated Principal Point", Photogrammetria, No. 2 (1950-1951).

2. Merritt, E. L., "Introduction to Camera Calibration", Technical Bulletin No. 127-50, U.S. Naval Photographic Interpretation Center, U.S. Naval Receiving Station, Washington 25, D. C., 1950.

BIBLIOGRAPHY (concluded)

3. Merritt, E. L., "Star Exposure Method of Camera Calibration", Technical Bulletin No. 131-50, U.S. Naval Photographic Interpretation Center, U.S.N. Receiving Station, Washington 25, D. C., 1950.

4. Rowley, J. C., and Schmidt, E., "A Rectification Transformation for Tilted Photographs", Univ. of Mich., Ann Arbor, Eng. Res. Inst. Project 1699, 1951.

5. Schmidt, E., "Tilt by Area Distortion", Univ. of Mich., Ann Arbor, Eng. Res. Inst. Project 1699, 1952.

6. Rowley, J. C., "Report on Camera Calibration", Univ. of Mich., Ann Arbor, Eng. Res. Inst. Project 1699, 1951.

7. Livingston, R. G., "Tangential Distortion in the Metrogon Lens", Report on Project 8-36-01-002, Engineering Research and Development Laboratories, Aerial Photographic Branch, Wright-Patterson Air Force Base, Ohio, October 20, 1950.

8. Sewell, Eldon D., "Field Calibration of Aerial Mapping Cameras", Photogrammetric Engineering, September, 1948.